Origin and timing of late diagenetic illite in the Permian–Carboniferous Unayzah sandstone reservoirs of Saudi Arabia

Stephen G. Franks and Horst Zwingmann

ABSTRACT

Diagenetic illite is one of two major porosity occluding cements in the Unayzah sandstone reservoirs (Permian–Carboniferous) of Saudi Arabia. The other is diagenetic quartz. This article focuses on the origin of illite and its timing. Illite has been formed by a reaction of detrital K-feldspar and early diagenetic kaolinite as temperatures increased due to burial. When either of the two reactants is exhausted, illite ceases to precipitate. There is no evidence that hydrocarbon emplacement, deep brine migration, or unique thermal events are factors in illite precipitation. Modeling of illite precipitation as a kinetically controlled reaction using burial histories of the samples studied generally yields a reasonable match between measured and modeled ages and amounts of illite. This lends further support to the gradual formation of illite over a time-temperature interval. Although quartz overgrowths and diagenetic illite may occur in the same thin section, they appear to be mutually exclusive locally. Quartz overgrowths do not occur on detrital quartz grains that are coated with diagenetic illite, and illite is rarely observed on quartz overgrowths. Therefore, it appears that not only does diagenetic illite inhibit nucleation of quartz overgrowths but quartz overgrowths may also inhibit precipitation of diagenetic illite. The two cements appear to compete for surface area on uncoated detrital quartz grains.

Manuscript received August 24, 2009; provisional acceptance January 12, 2010; revised manuscript received February 14, 2010; 2nd revised manuscript received March 15, 2010; final acceptance April 21, 2010.
DOI:10.1306/04211009142

AUTHORS

STEPHEN G. FRANKS ~ *Saudi Aramco Advanced Research Center, Dhahran, Saudi Arabia; present address: 7002 Wellington Point Road, Mckinney, Texas 75070; franks_steve@hotmail.com*

Stephen Franks received his Ph.D. in geology from Case Western Reserve University. He worked for Atlantic Richfield Corporation (ARCO) from 1974 to 1999, after which he formed a consulting company, RockFluid Systems, Inc., in Dallas, Texas. In 2001, he accepted a position with Saudi Aramco's Advanced Research Center. He retired from Saudi Aramco in April 2009 and now consults in Dallas.

HORST ZWINGMANN ~ *Commonwealth Scientific and Industrial Research Organization Earth Science and Resource Engineering, P.O. Box 1130, Bentley, WA 6102, Australia; and School of Earth and Environment, University of Western Australia, 35 Stirling Highway, Crawley, WA 6009, Australia; horst.zwingmann@csiro.au*

Horst Zwingmann is a principal research scientist at CSIRO and an associate professor at the University of Western Australia, Perth. He completed his Ph.D. at the University Louis Pasteur Strasbourg, France, in 1995. His research interests include isotopic dating and tracing of diagenetic processes in relation to petroleum exploration and clastic sedimentary systems.

ACKNOWLEDGEMENTS

We thank the Saudi Aramco management for the permission to publish this work. Ahmed Raza Yasim (Saudi Aramco Resource Assessment Group) kindly provided information on the hydrocarbon- and water-bearing intervals in the wells from which illite was dated. Pierre Van Laer and Khaled Arouri provided information on the time of hydrocarbon migration and trapping. Khalid Shahab, Saudi Aramco, provided the SEM images. The authors thank Ali Zharani (Geological Technical Services Division) and his team at the Saudi Aramco Core Storage facility for being helpful in laying out cores and helping

with sampling and shipping. Almost daily discussions with colleagues Clemens Van Dijk, Bill Carrigan, Salem A-Shammari (Saudi Aramco Advanced Research Center), and numerous other Saudi Aramco employees working the Unayzah have influenced this work through discussions over the years. The latter include John Melvin, Roger Price, Muhittin Senalp, Osama Suliman, Josh Cocker, and Chris Heine and Ron Sprague. Andrew Todd, CSIRO, is thanked for technical assistance. AAPG reviewers Joanna Ajdukiewicz, David Awwiller, Jens Jahrens, Dave Pevear, and Rob Lander provided insights and constructive criticism that significantly improved the manuscript. Steve Hill of IRES, Ltd. conducted most of the petrographic point counting.
The AAPG Editor thanks the following reviewers for their work on this article: David Awwiller, Jens Jahren, David Pevear.

INTRODUCTION

Permian–Carboniferous Unayzah sandstones are major oil and gas reservoirs in east central Saudi Arabia. Gas and condensate are produced from these deep sandstone reservoirs around the southern end of the huge Ghawar structure, mostly known for its prolific production of oil from younger carbonate reservoirs. Light, sweet oil is produced from shallow Unayzah fields of central Arabia near the basin margin southwest of Ghawar (Figure 1). Sandstones, siltstones, and minor shales of the Unayzah reservoir were deposited over a period of some 50 m.y. from the Late Carboniferous to the Middle Permian (Figure 2). At the beginning of Unayzah deposition, the Arabian plate lay at high south latitudes, perhaps as high as 75° south based on preliminary Saudi Aramco paleomagnetic data (J. Melvin, 2007, personal communication), but by the time the overlying Permian Khuff carbonates were deposited, the plate had moved northward to tropical latitudes. Sediments of the Unayzah, therefore, were deposited under a variety of climatic conditions and in a wide variety of depositional settings, from glacial outwash plains in the Unayzah C to melt-out glacial lakes and fluvial settings in the Unayzah B, to hot and arid desert sandstones of the Unayzah A, and finally to near-shore marine and estuarine settings in the more warm and humid basal Khuff clastics (BKC).

Present-day porosity and permeability in the Unayzah reservoir are a function of depositional, early postdepositional, and burial diagenetic factors. Variation in grain size and sorting, early pedogenesis, and cementation by quartz overgrowths and late diagenetic illite cements during deeper burial are the most important factors affecting current reservoir quality. The purpose of this article is to discuss the origin and timing of late diagenetic illite in the Unayzah. Pedogenesis and quartz cementation are beyond the scope of this article and will be addressed in future publications.

STRATIGRAPHY

The Unayzah reservoir is composed of several different, informal stratigraphic units separated by hiatuses of varying magnitude. These informally defined units are, from the top, the Basal Khuff Clastics (BKC), Unayzah A, Unayzah B, and Unayzah C. Recently, Melvin and Sprague (2006) identified an unconformity-bound member within the Unayzah B, which they refer to as the unnamed middle Unayzah Member (Figure 2).

Log correlations are difficult, and biostratigraphic control is sparse in the Unayzah. Palynomorphs are sometimes recovered

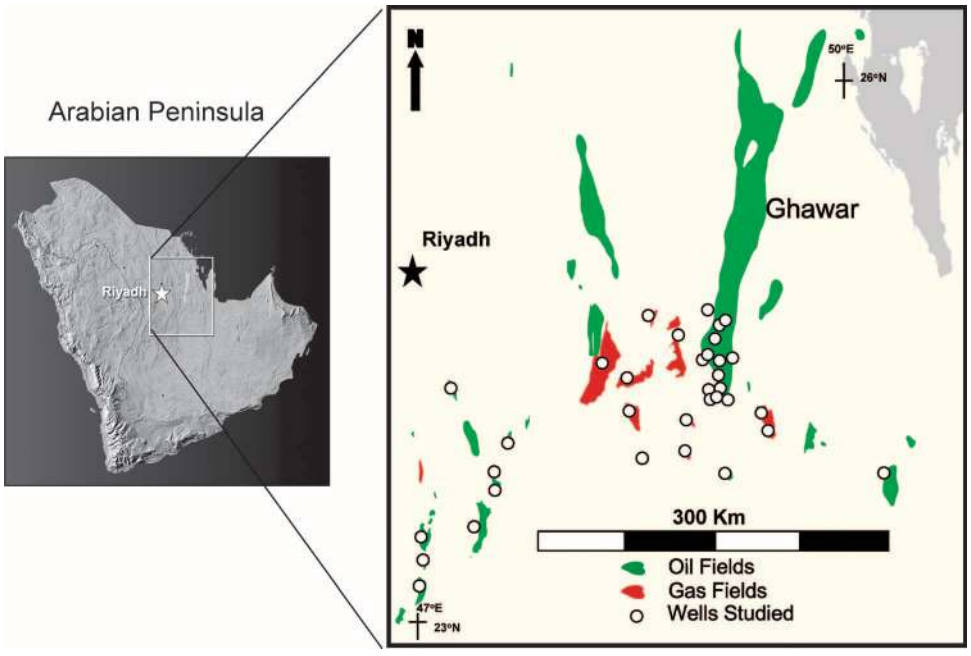

Figure 1. Location map showing the studied wells and major oil and gas fields. The large Ghawar structure has Unayzah production on the south end but produces primarily from younger carbonates.

from shaly intervals in the Unayzah B and BKC. These provide what little age control there is for the interval. The recent discovery of biosiliceous particles (phytoliths?) in the Unayzah may ultimately help provide a means of biostratigraphic subdivision (Garming et al., 2010). For a more detailed discussion of the age and historical evolution of the stratigraphic nomenclature of the Unayzah, the reader is referred to the work of Melvin and Sprague (2006) and references therein.

The lowest stratigraphic unit, the Unayzah C, rests on the Hercynian unconformity, a major hiatus in Saudi Arabia separating Carboniferous and younger sediments from rocks of Devonian and older ages. The younger pre-Khuff unconformity (PKU) (Figure 2) is also a significant unconformity. At some locations, the Unayzah A, B, and C are completely eroded, and the PKU merges with the Hercynian unconformity.

Resting on the PKU, sandstones, siltstones, and shales of the BKC represent the last major clastic influx of the Paleozoic and are followed by deposition of the overlying middle to Late Permian Khuff carbonates. Although a major unconformity, the PKU, separates the BKC from the Unayzah A, B, and C, the BKC is commonly informally included along with the underlying clastics in the so-called Unayzah reservoir interval.

AUTHIGENIC ILLITE GEOCHRONOLOGY

Comprehensive summaries concerning illite K-Ar dating can be found in Hamilton et al. (1989, 1992),

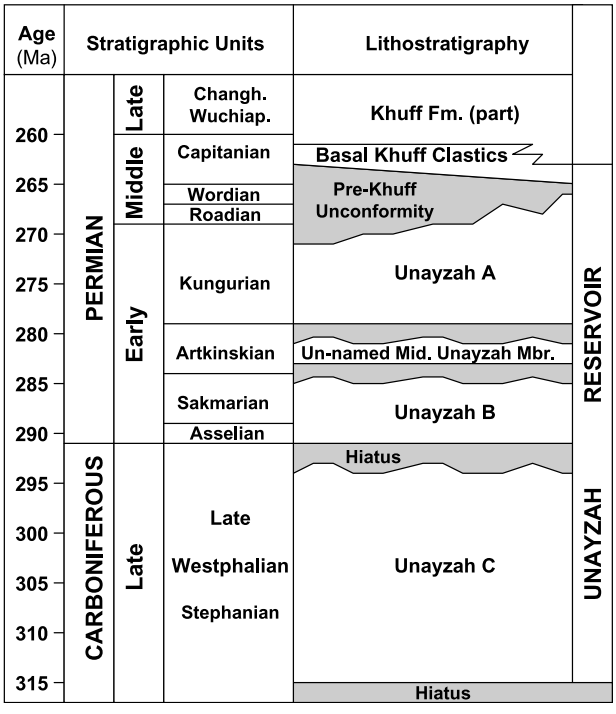

Figure 2. Stratigraphic column showing informal divisions of the Unayzah reservoir and assumed ages (modified from Melvin and Sprague, 2006).

Clauer and Chaudhuri (1995), Worden and Morad (2003), Meunier and Velde (2004), and Meunier et al. (2004). Authigenic illite in sandstones contains potassium and is therefore suitable for age determination using the K-Ar geochronometer (Pevear, 1999). Diagenetic illite is of interest for the petroleum industry because it can provide a K-Ar date constraining a heating event within a sedimentary basin. Dating of K-bearing illite minerals, using the K-Ar isotopic systems, offers the prospect of establishing the absolute timing of diagenetic events.

As outlined in numerous studies (see for example Clauer and Chaudhuri, 1995; Meunier and Velde, 2004, and references within), the radiogenic isotope systematics of sedimentary rocks are complex due to the intimate mixture of minerals of different origins such as detrital phases, potentially from a variety of sources, as well as authigenic minerals. Consequently, unambiguously interpreting measured ages is commonly difficult. Special sample preparation techniques involving freeze-thaw disaggregation to avoid overcrushing and extensive size separation to reduce the amount of detrital phases can address these issues (Liewig et al., 1987).

Progressive size reduction down to submicron-size fractions (<0.1 μm or finer) normally increases the proportion of authigenic clay phases in the clay component and minimizes contamination. Therefore, we generally assume that the most reliable isotopic ages for authigenic clay minerals are obtained for the finest size fractions. For neocrystallized illite, the finest separated particle size is derived from the ends of filamentous grains and should represent the most recently grown illite in sedimentary rocks (Lee et al., 1985). Conversely, coarser size fractions formed earlier during the illite formation process should yield older ages. However, evidence shows that illite can recrystallize and coarsen by Ostwald ripening processes in some burial sedimentary systems with conditions similar to the reservoirs investigated in this study (Eberl and Środoń, 1988; Eberl et al., 1990). This process, however, is questioned in later articles (e.g., Środoń et al., 2000). In reality, grain-size fractions of new-grown illite are mixtures of illite particles formed at different times during growth, and this growth history is commonly investigated by dating a range of different grain-size fractions.

Clauer et al. (1992) described in detail the influence of analytical problems and the investigator factor on illite age dating. Pevear (1999) suggested a new approach to estimate the ages of the detrital and diagenetic end members by (1) quantitatively determining via x-ray diffraction (XRD) the amount of the end members in different size fractions and (2) by plotting the points (normalized to 100%) as apparent K-Ar age vs. percent of detrital illite, and linearly extrapolating to 0 and 100% detrital to evaluate the end-member ages (illite age analysis). In this model, the extrapolated diagenetic age is the mean (integrated) age of the time interval over which illite formed.

In addition, the validity and importance of the assumptions involved in K-Ar dating of authigenic illite (e.g., contamination, closed system behavior, excess Ar) must be carefully addressed and the sample material characterized using a wide range of tools comprising XRD, scanning electron microscopy (SEM) and x-ray diffraction (XRD), particle granulometry, and transmission electron microscopy (TEM). Illite formation is dependent on several parameters, including temperature and pressure ranges and formation fluid chemistry. These parameters are discussed in detail for the North Sea Brent Group by Hamilton et al. (1992). Variables that control the rate of illite growth range from temperature, pressure, concentration of reactants (mainly K, Si), rate of supply of reactants, pore-fluid velocity, rate of diffusion or active fluid flow, time to the presence of an aqueous pore fluid, and nucleation surface area.

METHODOLOGY

Thin sections were made from 650 core plugs (or trim ends from the plugs) on which unstressed helium porosity and air permeability had been previously measured. Three hundred counts per section were made for composition, and 100 counts per section were made for grain size and sorting. Sorting was also visually estimated. Because of the high microporosity of diagenetic illite, a subset of samples was analyzed by XRD to correct for porosity

within the point-counted volume percent illite. Qualitative determination of illite composition was made using energy dispersive analysis (EDAX).

Six matrix-free sandstones were selected for K-Ar dating of diagenetic illite. All samples were crushed into chips with a maximum dimension of less than 10 mm (0.3 in.) by a hammer and then gently disaggregated using a repetitive freezing and thawing technique to avoid artificial reduction of rock components and contamination of finer size fractions with K-bearing minerals such as K-feldspar (Liewig et al., 1987). Grain-size fractions less than 2 μm were separated in distilled water according to Stokes' law, and the efficiency of the separation was monitored by a laser particle sizer. Additional grain-size fractions of less than 0.1 and 0.4 μm were obtained using a high-speed centrifuge. Because of the sample nature, separating a sufficient less than 0.1 μm from all samples was not possible.

The mineralogy of the size fractions was determined by XRD. The identification and analysis of clay minerals have been summarized by Moore and Reynolds (1997). Diffractograms were obtained from air-dried slides and analyzed with a Philips X'Pert x-ray diffractometer fitted with Cu x-ray tube running at 40 kV per 40 mA and a graphite monochronometer in the diffracted beam path to select CuKα radiation. Samples were scanned over the range of 2theta = 3–60° at 0.015° 2theta/s. Glycolated XRD analyses were conducted to investigate the potential occurrence of expandable mixed layer smectite mineral content.

For SEM investigations, freshly broken rock surfaces of sample chips from core samples were carbon coated and examined in secondary electron mode using a Philips 300 SEM equipped with an energy dispersive system (EDS) x-ray analyzer. The SEM principles and applications are summarized in many publications (see, for example, Murr, 1982). In addition, a JEOL 2010 TEM (200 kV) was used for detailed grain-by-grain characterization of the less than 0.1- and less than 0.4-μm clay mineral fractions as suggested by Hamilton et al. (1989). Clay-particle morphologies were investigated as well as the grain-size distribution within the fractions. An introduction into TEM investigations of clay minerals can be found in the work of Sudo et al. (1981). One drop of clay solution was loaded on a microcarbon grid film and dried under air. The mineralogy of individual particles was investigated by an attached EDS.

The K-Ar dating technique follows standard methods described in detail elsewhere (Dalrymple and Lanphere, 1969; Faure 1986). The potassium content of each sample was determined in duplicate by atomic absorption, and the pooled error of samples and standards is better than 2%. Argon isotopic determinations were performed using a procedure similar to that described by Bonhomme et al. (1975). Samples were preheated under vacuum at 80°C for several hours to reduce the amount of atmospheric argon adsorbed onto the mineral surfaces during sample handling. Argon was extracted from the separated mineral fractions by fusing the samples within a vacuum line serviced by an on-line ^{38}Ar spike pipette. The isotopic composition of the spiked argon was measured with a high-sensitivity on-line VG3600 mass spectrometer. The ^{38}Ar spike was calibrated against biotite GA1550 (McDougall and Roksandic, 1974). Blanks for the extraction line and mass spectrometer were systematically determined, and the mass discrimination factor was determined periodically by air measurements (Table 1). About 25 mg of sample material was required for argon analysis.

During the study, several international age standards were analyzed. The results are summarized in Table 2. The error for argon analyses is below 1%, and the average $^{40}Ar/^{36}Ar$ value of the air measurements yielded 295.45 ± 0.21. The K-Ar ages were calculated using ^{40}K abundance and decay constants recommended by Steiger and Jäger (1977). The age uncertainties consider the errors during sample weighing, $^{38}Ar/^{39}Ar$ and $^{40}Ar/^{38}Ar$ measurements, and K analysis. The K-Ar age errors are within 2 sigma uncertainty (Table 2).

PETROLOGY

Most sandstones in the Unayzah reservoir are quartz arenites with a lesser proportion of subarkosic and rarely arkosic sandstones. In all units, the feldspar content increases with decreasing grain size (Figure 3),

Table 1. K-Ar Standards and Airshot Data

CSIRO* ID	K (%)	Rad. ^{40}Ar (mol/g)	Rad. ^{40}Ar (%)	Age (Ma)	Error (Ma)	Difference from Recommended Reference Age (%)
LP6-89	8.37	1.9130×10^{-9}	97.52	127.18	1.83	–0.56
GLO-102	6.55	1.1116×10^{-9}	95.20	95.28	1.44	+0.26
HD-B1-76	7.96	3.3826×10^{-10}	93.08	24.35	0.36	+0.58
GLO-103	6.55	1.1058×10^{-9}	92.91	94.80	1.46	–0.24

Airshot ID	$^{40}Ar/^{36}Ar$	+/–
AS71-AirS-1	295.45	0.19
AS71-AirS-2	294.90	0.22
AS72-AirS-2	295.24	0.11
AS72-AirS-3	295.67	0.30
AS72-AirS-4	295.97	0.23

*CSIRO = Commonwealth Scientific and Industrial Research Organization.

and very fine sandstones and siltstones can be quite feldspathic. K-feldspar is the dominant feldspar (up to 21%) in Unayzah sandstones; plagioclase is a persistent but minor (1–3%) background phase in most samples.

Unayzah C sandstones are the most quartz rich of all Unayzah reservoir units (Figure 4). This is in part because Unayzah C sandstones are, on average, coarser grained. They are moderately to poorly sorted, and grain sizes range from very fine to very

Table 2. The K-Ar Ages of Diagenetic Illite of Different Size Fractions Separated from Unayzah A Sandstones*

Sample	Size Fraction (μm)	K (%)	Rad. ^{40}Ar (mol/g)	Rad. ^{40}Ar (%)	Age (Ma)	Error (Ma)
Well A 13,776.7 ft (4200 m)	<0.4	7.14	1.5230×10^{-9}	96.75	119.0	2.4
	<2	7.24	1.5401×10^{-9}	97.58	118.7	2.4
	2–6	6.78	1.5513×10^{-9}	97.97	127.3	2.6
Well A 13,781.0 ft (4202 m)	<0.4	6.86	1.3980×10^{-9}	95.99	113.8	2.3
	<2	6.95	1.4046×10^{-9}	94.49	112.9	2.3
	2–6	6.54	1.5396×10^{-9}	96.72	130.9	2.6
Well B 14,392.0 ft (4388 m)	<0.1	7.50	1.4262×10^{-9}	94.09	106.4	2.2
	<0.4	7.37	1.4703×10^{-9}	97.49	111.5	2.3
	<2	7.61	1.4210×10^{-9}	92.87	104.6	2.1
	2–6	7.08	1.5244×10^{-9}	96.62	120.1	2.4
Well C 13,694.2 ft (4175 m)	<0.4	7.33	1.3434×10^{-9}	97.91	102.7	2.1
	<2	6.61	1.2253×10^{-9}	96.95	103.8	2.1
	2–6	5.71	1.1233×10^{-9}	97.34	110.0	2.2
Well D 15,073.7 ft (4596 m)	<0.1	7.19	1.2507×10^{-9}	92.81	97.6	2.0
	<0.4	7.09	1.2757×10^{-9}	94.16	100.9	2.0
	<2	6.82	1.1918×10^{-9}	96.45	98.0	2.0
	2–6	7.02	1.2341×10^{-9}	95.45	98.6	2.0
Well E 15,511.0 ft (4729 m)	<0.1	8.92	1.3581×10^{-9}	92.14	85.7	1.7
	<0.4	7.47	1.4586×10^{-9}	95.44	109.2	2.2
	<2	7.30	1.4089×10^{-9}	91.70	108.0	2.2
	2–6	7.17	1.3946×10^{-9}	94.47	108.8	2.4

*Samples from wells A, C, and D are from gas-productive sandstones. Samples from wells B and E are from nonhydrocarbon-bearing sandstones.

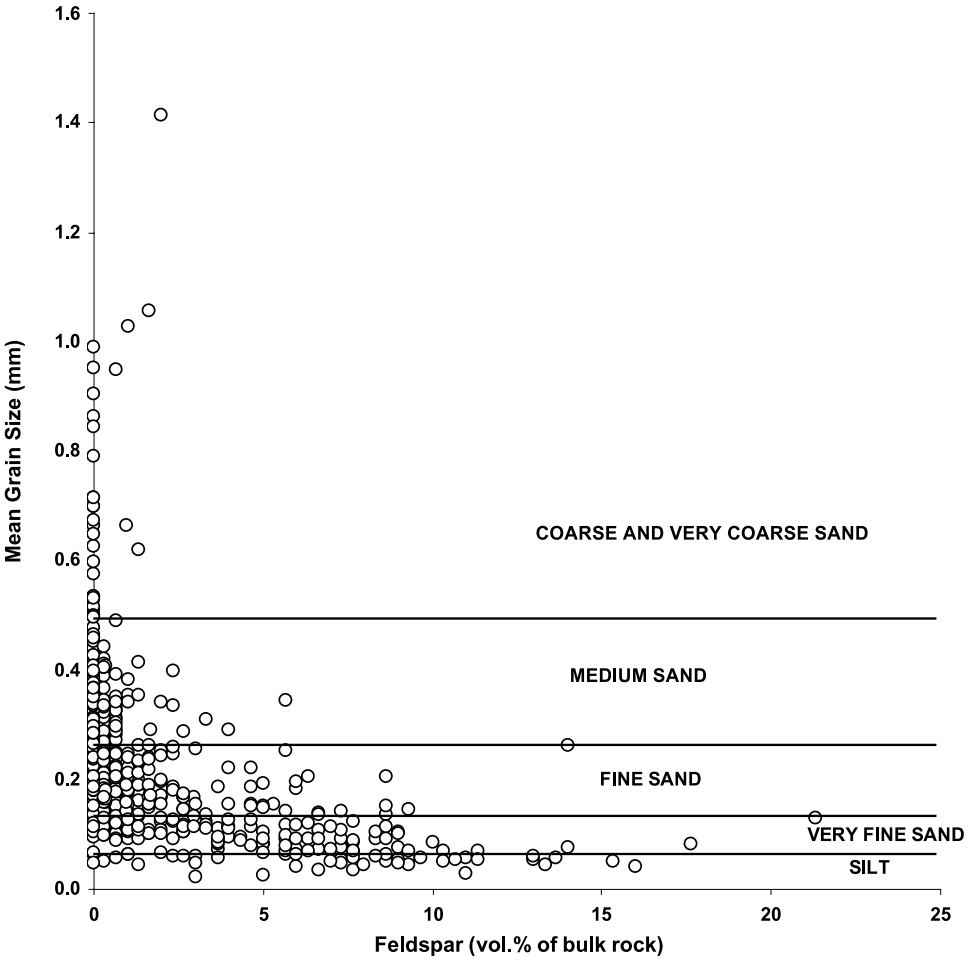

Figure 3. Mean total feldspar content from petrographic data versus mean grain size. Most feldspar is K-feldspar. Plagioclase is typically 1–2%. Feldspar increases significantly with decreasing grain size and is especially abundant in fine sandstones and siltstones.

coarse with a median grain size of 0.32 mm (0.01 in.). The sandstones are matrix poor and have little diagenetic illite compared to younger Unayzah units. The sandstones have the highest average percentage of quartz overgrowths (20%) of all Unayzah sandstones. Other characteristic features are abundant stylolites and microfractures. The sandstones are interpreted to have been deposited as glaciofluvial fans, braid plains, and eolian dunes in a periglacial environment (Senalp and Al-Duaiji, 2001) and as glacial outwash fans and high-energy braided streams (Melvin and Sprague, 2006).

The Unayzah B has a more variable detrital framework composition than the Unayzah C. Glaciolacustrine diamictites (Senalp and Al-Duaiji, 2001), in particular, contain a variety of plutonic, metamorphic, and sedimentary rock fragments. The most common lithic types are granite, quartz-mica schist, chert, and fine-grained micaceous and illitic sedimentary rock fragments. Felsic and mafic volcanic rock fragments are very rare. Rock fragments are most commonly found in rainout diamictites of the lower Unayzah B. The lower B has been suggested to represent a glacial retreat or melt-out phase (Senalp and Al-Duaiji, 2001; Melvin and Sprague, 2006).

Fluvial-lacustrine Unayzah B sandstones and siltstone are quartz arenites, subarkoses, and rarely arkoses (Figure 4). Arkosic sediments are mostly siltstones and very fine sandstones. The upper Unayzah B or the unnamed middle Unayzah Member of Melvin and Sprague (2006) is free of diamictites. Sandstones are similar in composition to the underlying Unayzah B; however, preliminary data suggest an increase in the plagioclase/K-feldspar ratio, perhaps because of the reduced chemical weathering accompanying the drying-out phase that reaches it culmination in the Unayzah A.

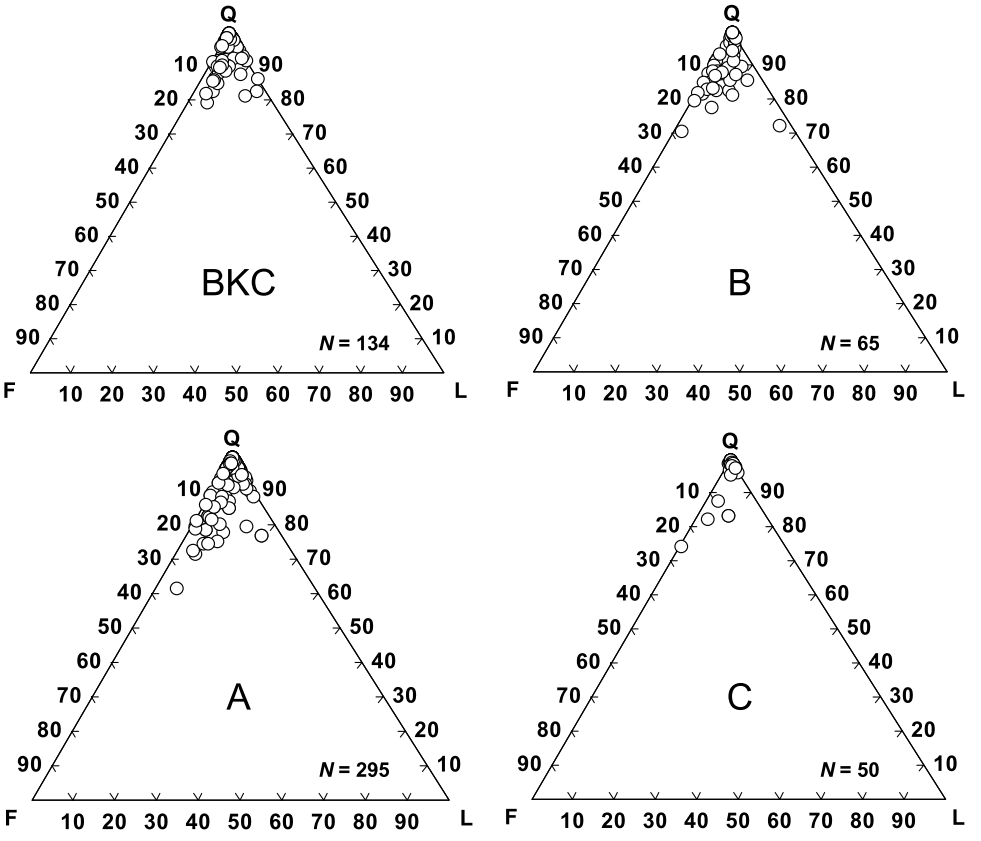

Figure 4. Normalized quartz (Q), feldspar (F), and lithic fragment (L) plots. The number of samples in each plot are basal Khuff clastics (BKC = 134), Unayzah A (295), B (65), and C (50). Most sandstones are quartz arenites or subarkoses. The Unayzah C is particularly rich in quartz arenites.

Unayzah A sandstones were deposited in a variety of desert environments: eolian dune, sand sheet, sabkha, playa, and fluvial (Senalp and Al-Duaiji, 2001). Framework composition is variable due to the control of grain size in the different environments (Figure 4). Feldspar is most abundant in very fine playa, fluvial sandstones and siltstones, and in the finer laminae of wind-ripple dune and sand-sheet sandstones. Upper fine and coarse sandstones of fluvial, eolian, and sabkha facies are predominantly quartz arenites.

The BKC sandstones are slightly more quartz rich than Unayzah A sandstones. Fluvial channel sandstones can be quite coarse, even pebbly. Pebbles consist mostly of chert, granite, and shale (rip-up clasts). Some fluvial channels contain medium to coarse subarkosic sandstones (mostly K-feldspar) with relatively fresh-appearing feldspars, suggesting a downcutting into a previously unexposed basement. The BKC sandstones were deposited mostly in fluviodeltaic to estuarine environments (the ash-Shiqqah Formation of Senalp and Al-Duaiji, 2001).

Infiltrated and illuviated clay coats (cutans) and early microquartz-grain coatings (Shammari and Shahab, 2002) are associated with paleosols in the Unayzah reservoir. The clay cutans commonly exhibit geopetal features and delicate layering or banding typical of illuviated soil clays. In most, but not all, cases, they are within intervals punctuated by incipient or well-developed paleosols. The clay coats are presently composed mostly of illite, but kaolinite and microcrystalline silica are locally present. They are dominant in some of the well-developed paleosol horizons in the upper part of the section.

Microquartz in the Unayzah consists of small (1–10 μm) euhedral quartz crystals coating the surfaces of detrital quartz grains. They are very similar in appearance to microquartz-grain coatings described by Aase et al. (1996) in the North Sea. The orientation of the *c* axes of the microquartz crystals has not been statistically determined, but they appear not to be entirely parallel. Quartz overgrowths or outgrowths occur only where breaks in the microquartz-grain coatings are present.

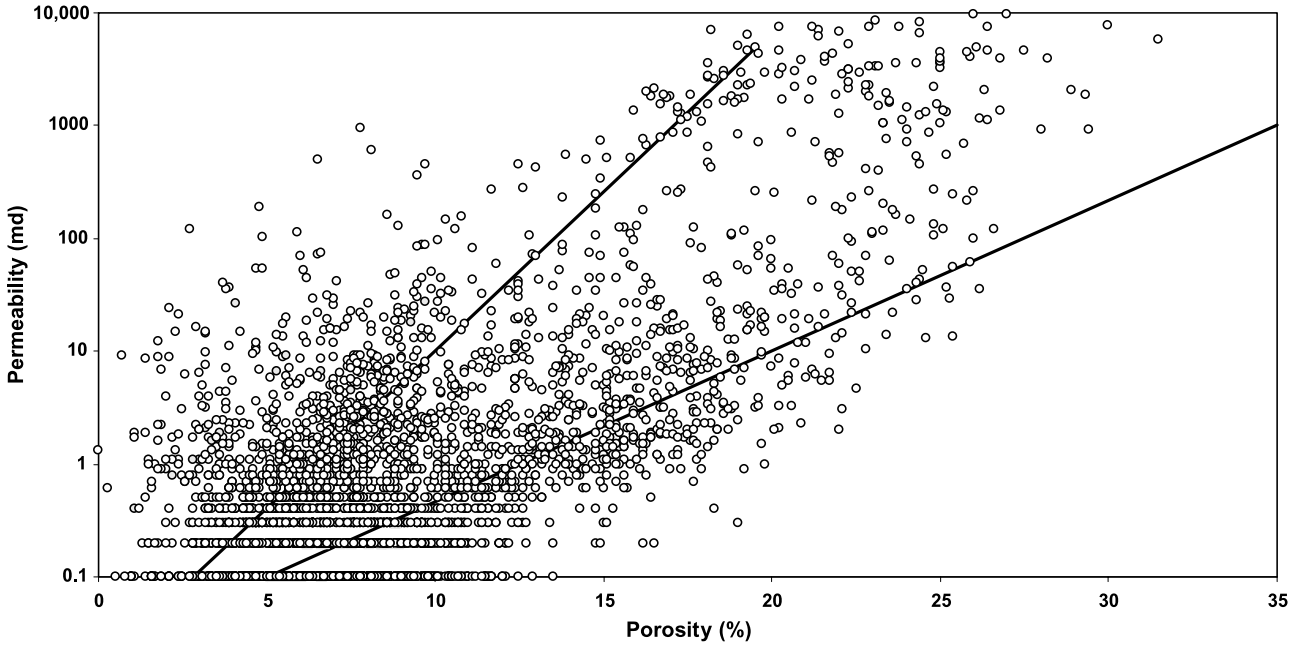

Figure 5. Unstressed porosity-versus-permeability plot for Unayzah sandstones. Upper and lower lines are derived from individual well plots, which show two distinct trends in many, but not all, wells. The upper line is a best-fit line for sandstones with an average grain size of 0.31 mm (0.012 in.), 16% quartz overgrowths, and 7% diagenetic illite. The lower line is for sandstones with an average grain size of 0.17 mm (0.006 in.), 12% diagenetic illite, and 7% quartz overgrowths.

Paleosols increase in abundance from the Unayzah C to the BKC. Following the terminology of Mack et al. (1993), oxisols, gleysols, argillisols, and vertisols are common in the BKC and indicate warm humid conditions with some drier periods. Silcretes are locally present in the BKC and the uppermost Unayzah A. Calcisols and protosols lower in the Unayzah A reflect more arid conditions. Paleosols in the Unayzah B are mostly argillisols and protosols. No definitive paleosols have been identified in the Unayzah C.

Franks (2008, and unpublished Saudi Aramco reports) suggested that the stratigraphic changes in paleosol abundance and type are a result of paleoclimatic changes that occurred as the Arabian plate moved from high southerly latitudes in the Unayzah C to more tropical latitudes during the BKC. The abundance of infiltrated and illuviatedw clay coatings also seems to reflect these climatic changes. On average, less than 15% of Unayzah C detrital quartz-grain surfaces are coated with infiltrated clay compared to more than 70% in the BKC. Details of the pedogenesis within the Unayzah and distribution of grain coatings are subjects of a future article.

RESERVOIR QUALITY AND RELATIVE TIMING

Quartz overgrowths and diagenetic flakey to fibrous illite are the dominant postdepositional controls on reservoir quality in the Unayzah. Figure 5 is a crossplot of unstressed helium porosity and air permeability of several thousand Unayzah core plugs from more than 40 wells. Although considerable scatter exists within the data, examination of poroperm plots from individual wells indicates that two general trends are present, shown by the two lines in Figure 5. Petrographic analysis of samples selected along each of the two trends demonstrates that the upper trend, which exhibits higher permeability for a given porosity, is composed dominantly of medium-grained quartz-cemented sandstones with a mean grain size of 0.31 mm (0.01 in.), mean quartz cement of 16%, and mean illite of 7%. The lower trend is dominated by finer grained sandstones with a mean grain size of 0.17 mm (0.006 in.), mean diagenetic illite of 12%, and mean quartz overgrowths of 7%. This trend of finer, illitic sandstones having a lower permeability for a given porosity than coarser, quartz-cemented sandstones is

not unique to the Unayzah and is, in the authors' experience, observed in many basins.

Fluid-inclusion data, illite age dating, and distribution of cements indicate that illite and quartz cement in the Unayzah formed over about the same time interval. Both illite and quartz increase with increasing depth of burial (Figure 6a, b). The observed increase in both illite and quartz occurs over approximately the same depth interval with the greatest increase between 10,000 and 12,000 ft (3048 and 3658 m). Present temperatures at these depths range from about 120 to140°C. Homogenization temperatures of aqueous fluid inclusions from quartz overgrowths in the Unayzah range from 70 to nearly 160°C but exhibit a broad peak in the range of 110–135°C (Figure 7). Burial histories indicate that Unayzah sandstones entered the quartz cementation window (~70°C) at 126–158 Ma, reaching the 110–135°C peak temperatures shown in Figure 7 about 68–117 Ma, depending on the location. They remain within the quartz cementation window today. Mean K/Ar dates of diagenetic illite (discussed below) range from about 85 to 118 Ma, indicating significant overlap with the time of quartz cementation.

Quartz overgrowths are inhibited by early-formed illuviated clay and microquartz-grain coatings. The best porosity and permeability in deep Unayzah reservoirs are commonly associated with one of these two scenarios. Both early clay coatings and microquartz-grain coatings are associated with pedogenic processes. Microquartz in Unayzah sandstones is associated with siliceous paleosols (silcretes and siliceous argillisols). Tangential clay coats are most abundant in sandstones associated with protosols, vertisols, argillisols, and oxisols.

Late diagenetic illite also protects otherwise uncoated detrital quartz grains from quartz nucleation and preserves porosity. This occurs particularly in eolian dune sandstones in which pedogenesis is typically less common. Quartz precipitates as typical, optically continuous quartz overgrowths on uncoated detrital quartz grains or as elongated outgrowths (also optically continuous) where breaks in the early grain coatings or later diagenetic illite exists.

Diagenetic illite is observed on all clay-coated and uncoated detrital grains (quartz, feldspar, and lithics) and on clay cutans and bridges. Minor amounts of diagenetic illite are observed between microquartz crystals in samples that have microquartz grain coats and where diagenetic quartz outgrowths have not yet achieved euhedralism (Figure 8). Diagenetic illite, however, is rarely present on euhedral faces of quartz overgrowths and outgrowths which have precipitated on detrital quartz grains.

These observations suggest a competition between quartz and illite for nucleation on uncoated detrital quartz-grain surfaces. Whether illite or quartz cement prevails in the competition for available surface area depends on the temperature and availability of reactants required for each mineral and on their relative rates of precipitation. In the Unayzah, petrographic observations indicate that a few (3–5%) percent of diagenetic illite is enough to coat most grains sufficiently to inhibit quartz cementation.

How much quartz cement is required to envelope detrital quartz grains sufficiently to inhibit illite cementation is less clear. Comparing just the very fine Unayzah sandstones, presumably those with sufficient initial K-feldspar to form diagenetic illite, sandstones with more than about 8% quartz cement (by volume) typically appear to have 0–5-wt.% diagenetic illite. Those with less than about 8% quartz overgrowths have diagenetic illite from 5- to 10-wt.% illite. We suggest that this may be about the amount of quartz cement that is required to cover most detrital quartz-grain surfaces, but additional work is needed to confirm this.

PREVIOUS STUDIES OF DIAGENETIC ILLITE

Diagenetic illite is one of the most common and certainly one of the most detrimental diagenetic cements in hydrocarbon reservoirs. As a result, numerous studies of its occurrence and origin exist. The following is a brief discussion of some of the more relevant published works.

The Permian Rotliegende sandstones of the North Sea share some similarities with the Unayzah sandstones of Saudi Arabia not only in approximate age and depositional setting but also in terms of diagenesis. The detrital mineralogy of both is similar,

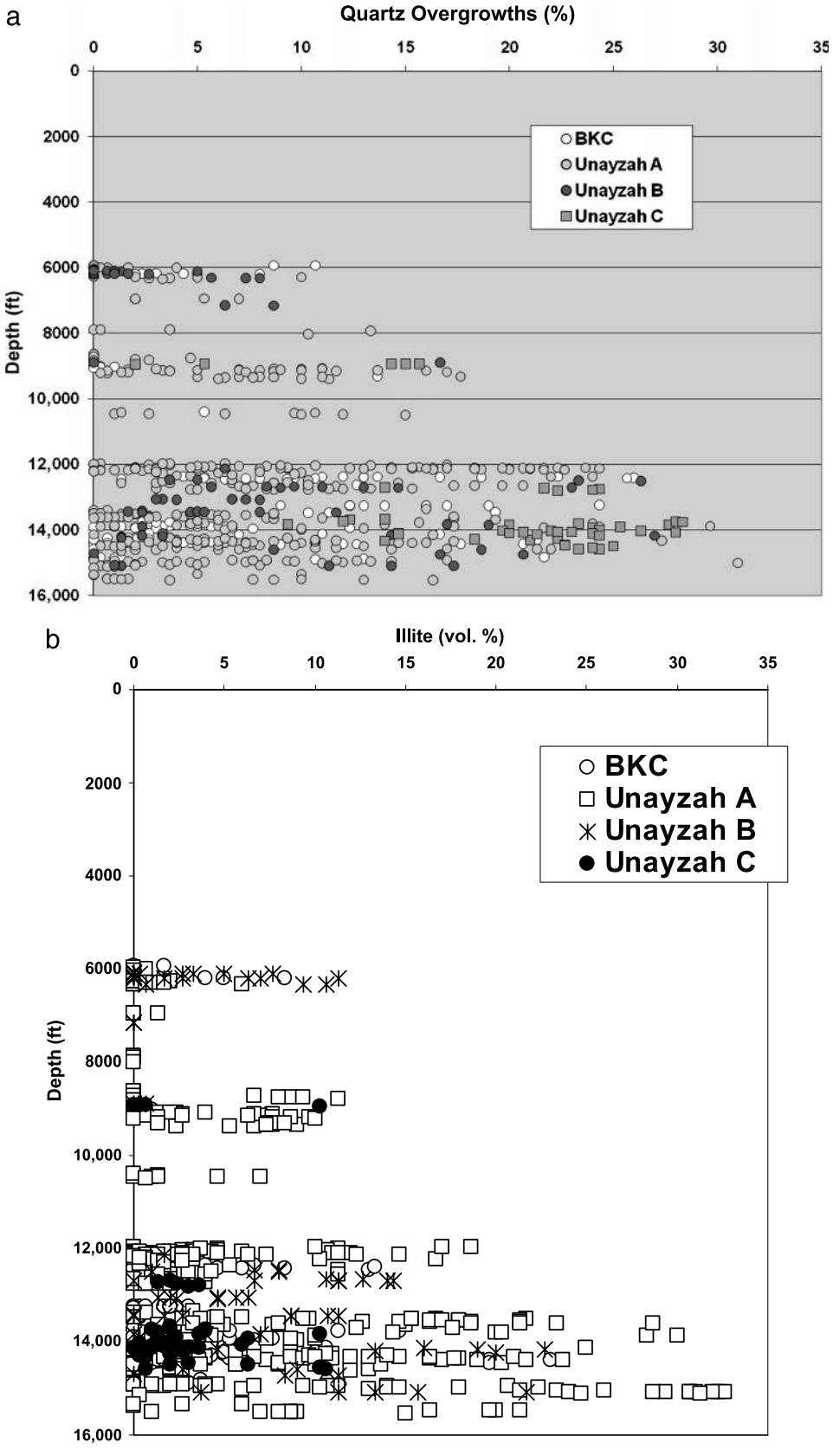

Figure 6. (a) Depth versus volume-percent quartz overgrowths determined from petrographic point counts. The Unayzah C has particularly high percentages of quartz overgrowths. (b) Depth versus volume-percent illite determined from petrographic point counts. Illite percentage does not include microporosity of approximately 70%. Unayzah C sandstones have particularly low percentages of diagenetic illite. BKC = basal Khuff clastics.

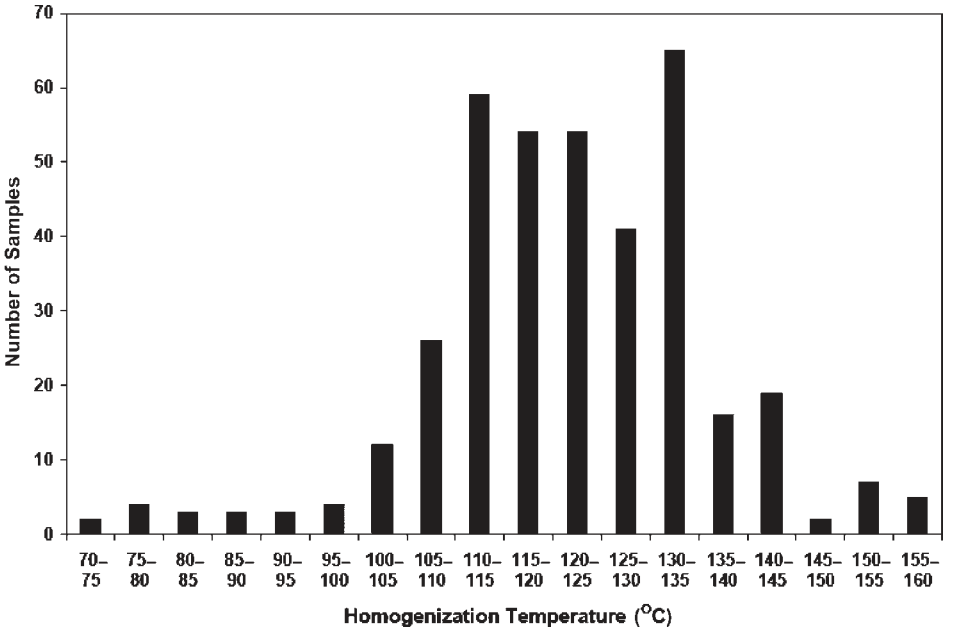

Figure 7. Homogenization temperatures for aqueous fluid inclusions in quartz overgrowths in Unayzah sandstones. Most fall in the 110–135°C range.

dominated by detrital quartz but with significant amounts of K-feldspar and lesser quantities of plagioclase. Mechanically infiltrated clays and clay bridges with geopetal structures are similarly observed in the Rotliegende, and diagenetic illite and quartz overgrowths are a major control of reservoir quality in both. Depositionally, the Rotliegende sandstones are more like the Unayzah A, having been deposited under desert conditions. No glacial (Unayzah B) or periglacial facies (Unayzah C) in the Rotliegende are observed.

Ziegler (2006) reviewed the previous 30 yr of published work on diagenetic illite occurrences in the Rotliegende sandstones of the North Sea and adjacent areas. She noted in her summary that illite in the Rotliegende has formed under burial diagenetic temperatures ranging from 20 to 140°C, but an examination of most articles she reviewed indicates that most illite forms at the higher end of this spectrum of temperatures.

Kaolinite is interpreted as an early diagenetic product formed by the decomposition of K-feldspar either by infiltration of meteoric water into the Rotliegende sandstones (Turner et al., 1993; Gluyas and Leonard, 1995) or by acidic pore water from Carboniferous coal measures expelled into the Rotliegende during burial (Gaupp et al., 1993; Platt, 1993).

Authors disagree about the mechanism of illite formation. Rossel (1982) called upon the illitization of earlier formed kaolinite by K-rich brines originating from evaporites in the section. In contrast, Turner et al. (1993) and Ziegler (1993) found no evidence for the illitization of kaolinite in Rotliegende sandstones and called for direct precipitation of illite from pore water. The precipitation is suggested to have been triggered by a change in pore-fluid

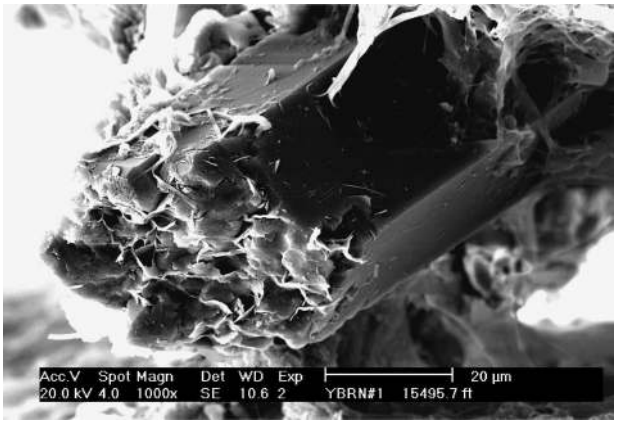

Figure 8. Scanning electron microscopy photograph showing diagenetic illite flakes and fibers growing on the noneuhedral end of a quartz outgrowth. Illite is also present on the detrital grain but almost absent on the crystal faces of the overgrowth. Illite is rarely observed on crystal faces of quartz outgrowths or overgrowths despite the generally coeval precipitation of illite and quartz.

chemistry or a thermal event (Ziegler, 2006). The suggestion of events, either fluid or thermal, commonly arises in published studies of illitization. The K-Ar dates from diagenetic illite have been used to determine the timing of these events (e.g., Lee, 1984; Lee et al., 1989; Platt, 1993; Robinson et al., 1993; Turner et al., 1993; Ziegler, 1993; Ziegler et al., 1994; Zwingmann et al., 1998, 1999).

Although the age and depositional setting of Jurassic sandstones in the North Sea are quite different from that of the Unayzah or Rotliegende, significant similarities in their diagenesis are also observed. Diagenetic illite and quartz overgrowths are the most important cements in many North Sea Jurassic reservoir sandstones. Evidence for early alteration of detrital K-feldspar to kaolinite and subsequent alteration of kaolinite to illite is observed. Ehrenberg and Nadeau (1989) described a gradual conversion of kaolinite to illite but with extensive illitization at depths of 3700 m (12,139 ft) where the present temperature is 140°C. They saw no difference in the degree of illitization in oil-saturated and water-saturated sandstones and concluded that water saturations of 20–30% must be sufficient to allow illitization to occur and that this implied diffusive transport of ions is essentially a closed system.

Other scientists who have conducted diagenetic studies of the North Sea Jurassic have also concluded that illite is formed by the reaction of kaolinite and K-feldspar in a closed system (Bjorkum and Gjelsvik, 1988; Chuhan et al., 2000, 2001). Chuhan et al. (2001) reported that the percentage of kaolinite and K-feldspar decreases markedly over the temperature interval of 120–130°C, with a corresponding increase in the percentage of diagenetic illite. The bulk-rock K_2O, however, shows no corresponding change over the interval, indicating that potassium released from K-feldspar alteration is retained in the rock. In a previous article, they showed that the amount of diagenetic illite is directly related to the initial amounts of K-feldspar available to react with kaolinite (Chuhan et al., 2000). They concluded that models of illitization must consider not only the burial and thermal history of sediments, but also the provenance which may determine whether a source of potassium for illitization in a closed system exists.

Exceptions to this closed-system interpretation are studies that have argued that illitization of kaolinite is associated with changes in pore-water chemistry accompanying oil migration (e.g., Hancock and Taylor, 1978; Sommer, 1978; Jourdan et al., 1987). In these cases, dating the time of diagenetic illite precipitation may be regarded as dating the time of hydrocarbon migration or trapping.

The origin of diagenetic illite in the Unayzah most closely parallels that described by Chuhan et al. (2000). As described in the following section, illite precipitation in the Unayzah appears to be a result of the reaction of kaolinite and K-feldspar in a relatively closed system. No special events, thermal or fluid, are required to explain the amount of illite, its distribution, or the K-Ar ages. No obvious relation of diagenetic illite precipitation to hydrocarbon generation or entrapment is observed.

ORIGIN OF DIAGENETIC ILLITE IN THE UNAYZAH

The primary focus of this article is on diagenetic flakey to fibrous illite, which coats grains, replaces kaolinite or feldspar, and reduces the reservoir quality of otherwise porous and permeable sandstones. Paleosols are common in the Unayzah, occurring in all units except the Unayzah C. More clayey paleosols began to punctuate the section in the time of late Unayzah A and BKC deposition as the climate became more humid (Franks, 2008, and unpublished Saudi Aramco reports). Illuviated, infiltrated, and depositional clays with a nondiagenetic, tangential habit are not addressed in this article. These clays most commonly are illitic and may have been illitized or recrystallized during burial, perhaps from smectite precursors.

Both fibrous and flakey illite have precipitated in Unayzah sandstones. Where both occur together, flakey illite always lies beneath fibrous illite, between it and the underlying grain surface, whether or not the grain has early grain coatings. Flakey illite grows out from the surfaces of detrital grains and has the appearance of radiating isopachous fibers in thin section. Although it might be argued that flakey illite is derived from earlier infiltrated

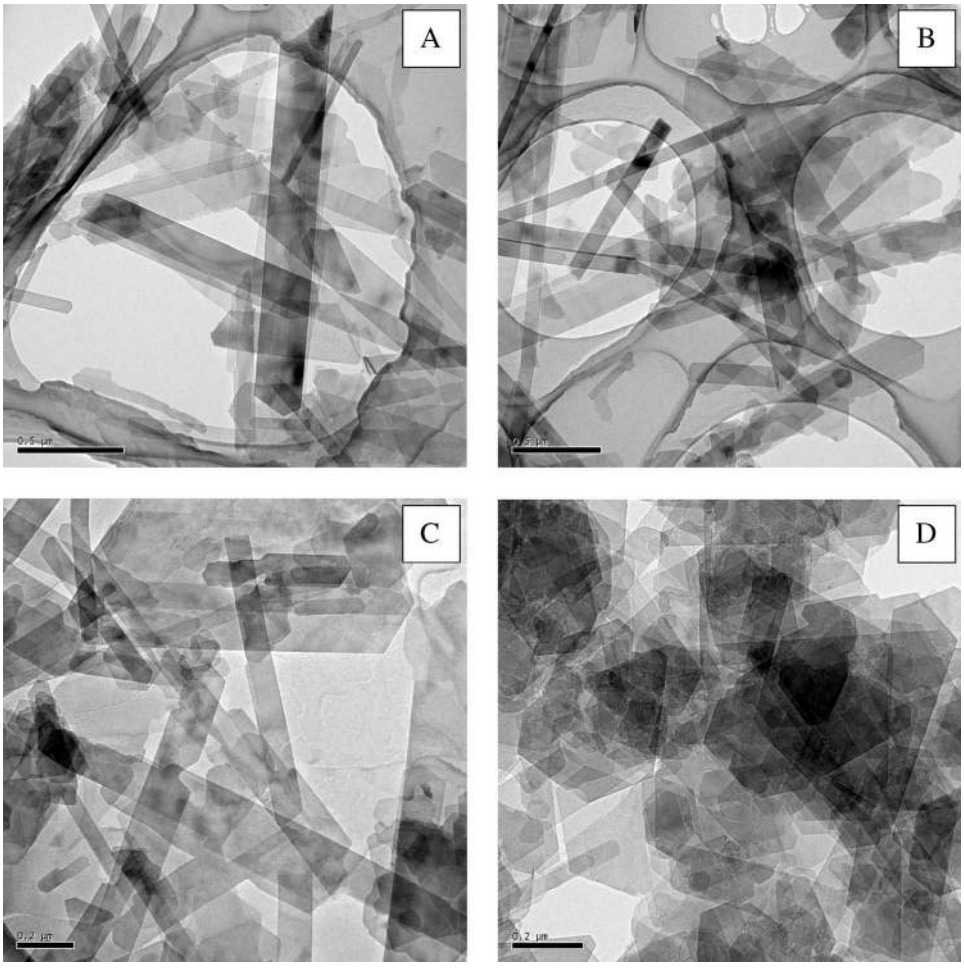

Figure 9. Transmission electron microscopy photographs of diagenetic illite.

clays, this does not appear to be the case. Numerous examples of sandstones with illuviated (now-illitic) tangential clay coats contain neither flakey nor fibrous illite in significant amounts. Also, flakey illite is common on otherwise uncoated detrital grains.

Although both flakey and fibrous illites are presumed to have been formed during burial diagenesis, we cannot rule out the possibility that flakey illite was originally an early diagenetic clay, perhaps smectitic, precipitated from early pore water and was converted to illite during burial by the well-documented smectite-to-illite reaction.

Fibrous illite in some cases appears to form as incipient extensions to the edges of the illite flakes, but in other cases, it has grown over the surfaces of the flakes from other nucleation sites on adjacent grains. Fibrous illite also forms isopachous rims a few microns thick on uncoated, detrital quartz grains. No attempt has been made to physically separate the two types for independent analysis. They are treated together here.

Figure 9 illustrates typical clay morphologies in the clay fractions observed by TEM. Some sample fractions contain aggregates of clay mineral particles. The TEM observations of the clay fractions document the occurrence of two distinct groups of particles: (1) idiomorphic illite fibers with elongated, well-crystallized grain edges and (2) idiomorphic platy illite flakes, together with hexagonal idiomorphic kaolinite with clear crystallized edges.

Illite, like K-feldspar, is more abundant in finer grained sandstones (Figure 10). It increases in abundance with increasing burial depth (Figure 6b), becoming especially abundant at depths greater than 12,000 ft (3658 m). This corresponds to present-day temperatures of about 130–140°C. Note in Figure 6b the much lower abundance of illite in the Unayzah C. The low amount of illite in the

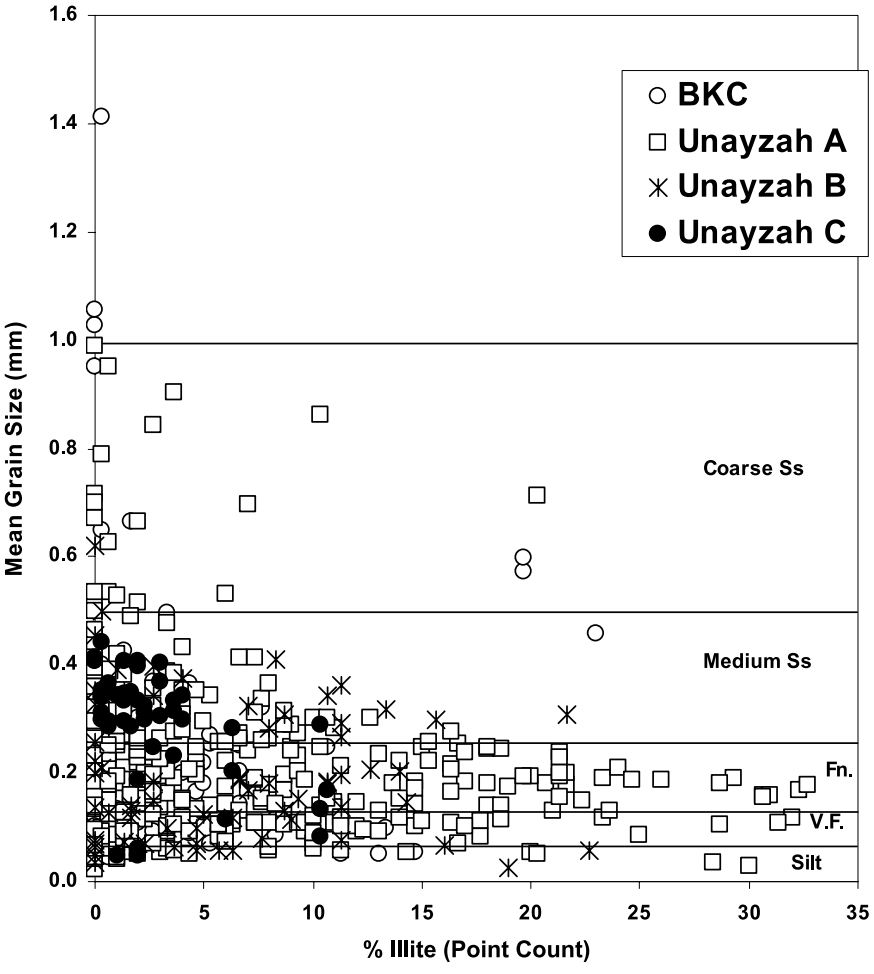

Figure 10. Petrographic volume-percent illite (uncorrected for microporosity) versus grain size. Illite, like K-feldspar, is much more abundant in finer grained sandstones (Ss) of the Unayzah but is much lower in the Unayzah C than other members.

Unayzah C where K-feldspar is also rare, and the abundance of illite in Unayzah units containing more K-feldspar suggests that illite formation is related to the presence of K-feldspar. In the Unayzah, K-feldspar is the most likely source of potassium within the sandstones, as other detrital K-bearing minerals (e.g., micas) are very rare.

Other potential sources of potassium for illite formation include pore waters. Potassium-rich brines have been called upon to initiate precipitation of diagenetic illite in some basins (e.g., Grathoff et al., 2001). Pore water in the deep Unayzah is highly saline and lies in the stability field of illite (Figure 11; Table 3). Despite this, sandstones in the Unayzah C, exposed to the same pore water as other Unayzah reservoir intervals, contain little diagenetic illite. Therefore, pore-water chemistry alone apparently is not a sufficient condition for illite precipitation in the Unayzah.

Petrographic evidence supports an origin of illite via a reaction of K-feldspar and kaolinite in a manner similar to that described by Chuhan et al. (2001) in the Garn Formation of the North Sea. Shallow Unayzah fields at present depths of 6000–8000 ft (1829–2438 m) where temperatures are less than approximately 100°C have little or no diagenetic illite. Detrital feldspars in these fields are strongly leached and altered partially or completely to kaolinite (Figure 12a) by early pedogenesis (Aktas and Cocker, 1996) and shallow groundwater leaching. With increasing burial and higher temperatures, early-formed kaolinite and remaining K-feldspar are gradually converted to flakey and fibrous illite (Figure 12b–d).

The formation of diagenetic illite at the expense of kaolinite and K-feldspar is not, however, readily evident in the depth distribution of K-feldspar and kaolinite (Figure 13a, b). Although average

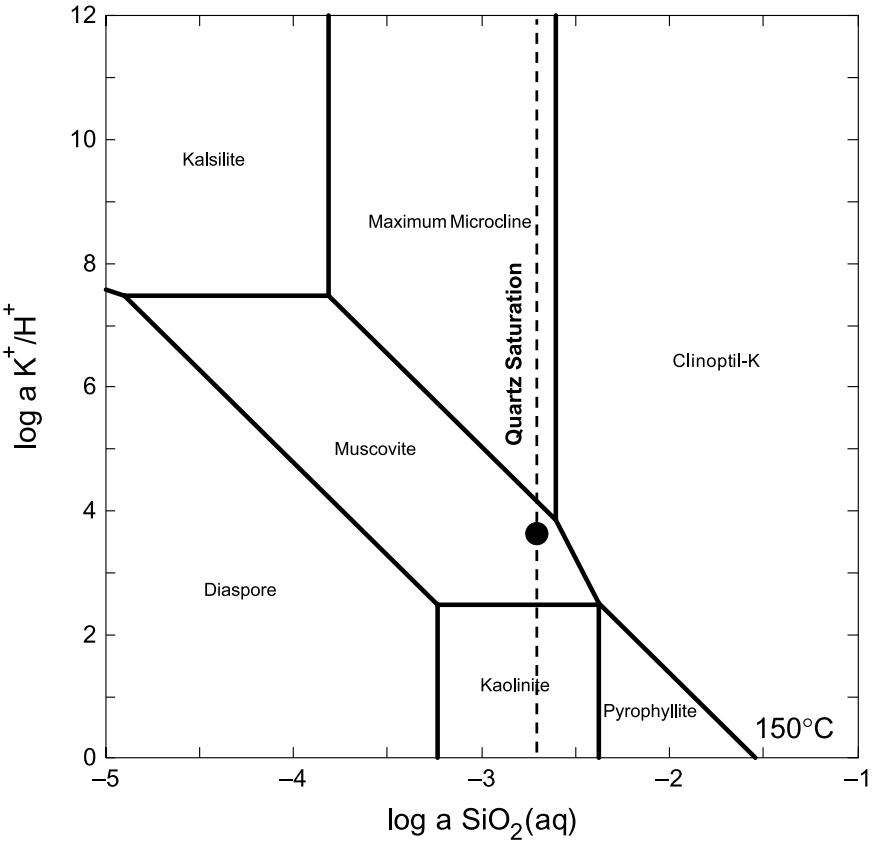

Figure 11. Activity-activity diagram of downdip Unayzah pore water from an extended flow test from a well at the south end of the Ghawar structure (Figure 1; Table 3). Pore water is within the stability field of muscovite (a proxy for illite) and approximately at quartz saturation.

abundances of both minerals decrease with depth, a wide variation in the percentages of K-feldspar and kaolinite is observed even in the deepest samples. When viewed in context of the proposed illite-forming reaction, however, these trends are readily explained.

$$Al_2Si_2O_5(OH)_4 + KAlSi_3O_8 \rightarrow KAl_3Si_3O_{10}(OH)_2 + 2SiO_2 + H_2O \quad \text{(reaction1)}$$

Although an idealized formula for illite is used in reaction 1 (EDAX analysis indicates that Unayzah illite actually contains both Fe and Mg substituting for Al), it serves to illustrate a point. As written, 1 mol of kaolinite and 1 mol of K-feldspar react to form 1 mol of illite (and 2 mol of quartz). Sandstone with equal molar amounts (m) of kaolinite and K-feldspar will, upon complete reaction, contain only illite with no remaining reactants (kaolinite or K-feldspar). However, a sandstone initially containing more moles (M) of one reactant than the other (m) will contain, after complete reaction, illite plus whichever reactant was present in excess.

(m)Kaolinite + (m)K–feldspar → (m)Illite
(equal moles; no remaining reactants)

(M)Kaolinite + (m)K–feldspar → (m)Illite + (M – m)Kaolinite
(residual kaolinite: feldspar limited)

(m)Kaolinite + (M)K–feldspar → (m)Illite + (M – m)K–feldspar
(residual K–feldspar: kaolinite limited)

Therefore, the variations of kaolinite and K-feldspar versus depth shown in Figure 13 are in part a result of the illitization reaction and the relative proportions of reactants prior to illitization. This is further illustrated by considering the relative amounts of product (illite) and reactants (kaolinite and K-feldspar) in the individual sandstones

Table 3. Chemical Composition of Unayzah Pore Water from an Extended Test of a Well Near Well C (Figure 15) Considered Typical of Downdip Unayzah Waters

Ion	mg/L	Ion	mg/L
Na	65,852	SO_4	<25
Ca	27,380	Cl	156,717
Mg	2321	HCO_3	16
K	3004	Br	2660
Si	20		
Sr	2123	TDS*	260,117

*TDS = total dissolved solids.

analyzed. This approach is very similar to that outlined by Chuhan et al. (2000).

Figure 14 shows ternary plots of the reactants, kaolinite and K-feldspar, and the product, diagenetic illite, in Unayzah A fine-grained, matrix-free (originally porous and permeable) sandstones from shallow, intermediate, and deep wells. Present-day temperature ranges are indicated, although some shallow fields have probably undergone uplift of a few kilometers since their deepest burial.

Sandstones in the shallowest fields (Figure 14a) show nonequilibrium, partly reacted, mixtures of kaolinite, K-feldspar, and illite in most samples. With increasing depth and temperature, most sandstones become equilibrium or near-equilibrium assemblages of either illite + K-feldspar or illite + kaolinite, the lesser reactant having been consumed (Figure 14b). Sandstones falling along the kaolinite-illite axis at the bottom of the ternary plot (Figure 14c) are those in which all K-feldspar has been consumed (feldspar limited). Those along the kaolinite-illite axis on the right side of the ternary plot are those in which all kaolinite has been consumed (kaolinite limited).

When kaolinite-limited and feldspar-limited samples are plotted as to their geographic locations, a pattern emerges (Figure 15). Sandstones in which the amount of diagenetic illite is limited by a shortage of K-feldspar occur in wells to the west-southwest of the south end of Ghawar; those limited by a shortage of kaolinite lie generally to the south and southeast of Ghawar. Either all sandstones initially had somewhat similar amounts of K-feldspar and those to the west-southwest (nearer the basin margin) had a higher percentage of the original feldspar altered to kaolinite during early diagenesis, or sandstones to the east-southeast of Ghawar initially had higher K-feldspar content, i.e., a provenance effect.

Evidences supporting early conversion of feldspars to kaolinite in the shallow fields are published

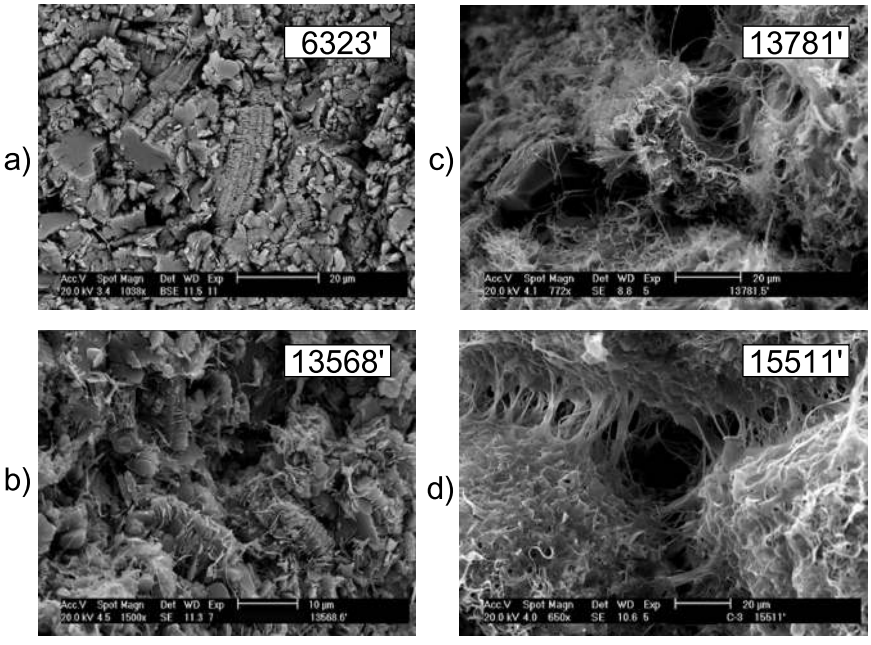

Figure 12. Secondary electron microscopy photographs of kaolinite-K-feldspar-illite at different depths. Photomicrographs show increasing illite with increasing depth (temperature) in the Unayzah. (a) Vermiform kaolinite booklets in the shallow Unayzah sandstone at 6323 ft (1927 m) with no illite; (b) vermiform kaolinite booklets at 13,568 ft (4135 m) with fibrous illite growths; (c) pore-filling flakey and fibrous illite partly in sandstones at 13,781 ft (4200 m); (d) fibrous and flakey illite lining and bridging pores in sandstone at 15,511 ft (4728 m).

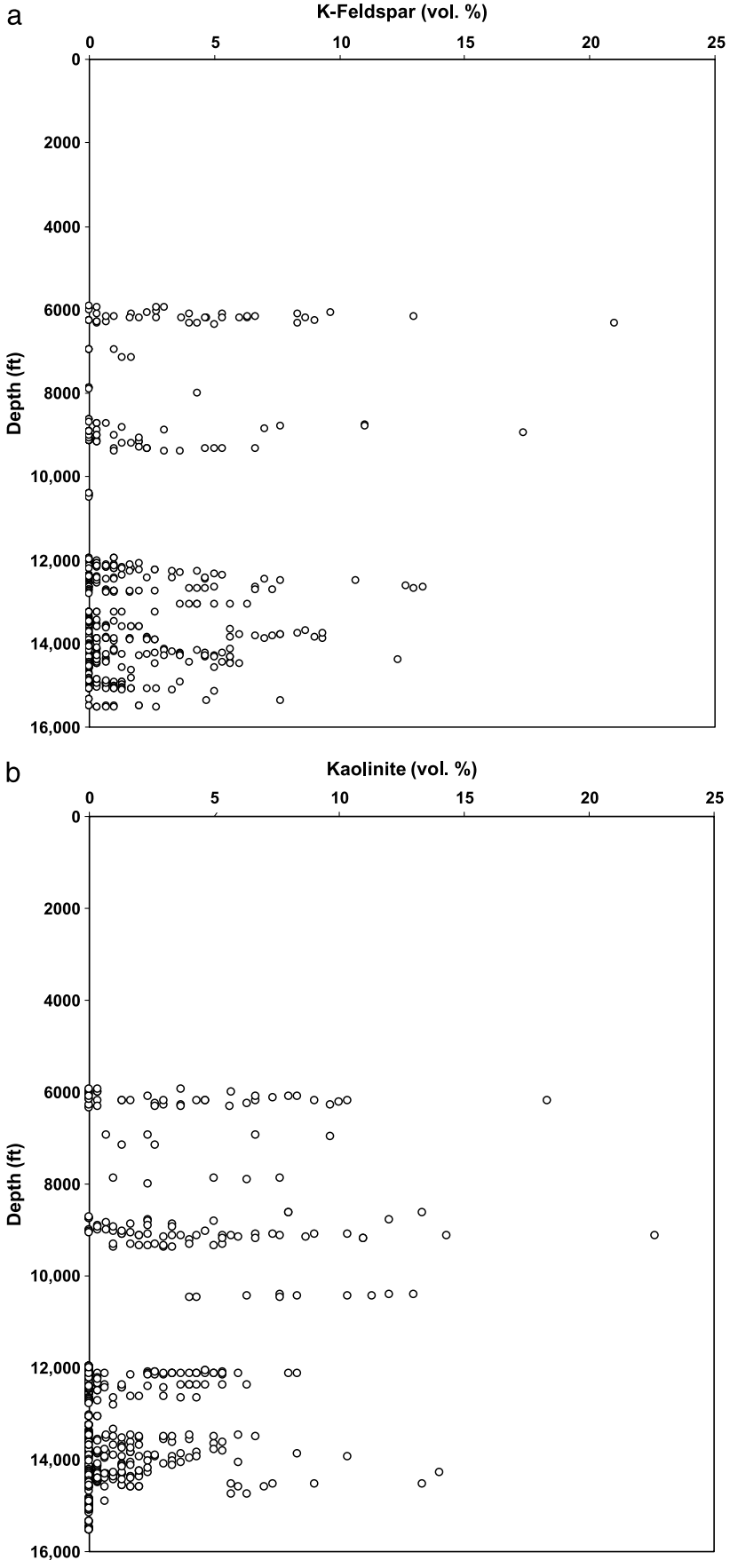

Figure 13. (a) Depth versus volume-percent K-feldspar from petrographic point counts. Although the K-feldspar content generally decreases with depth, considerable variation at all depths is observed. (b) Depth versus volume-percent kaolinite (petrographic point counts uncorrected for microporosity of ~50%). Although the average content of kaolinite decreases with depth, significant variation at all depths is observed.

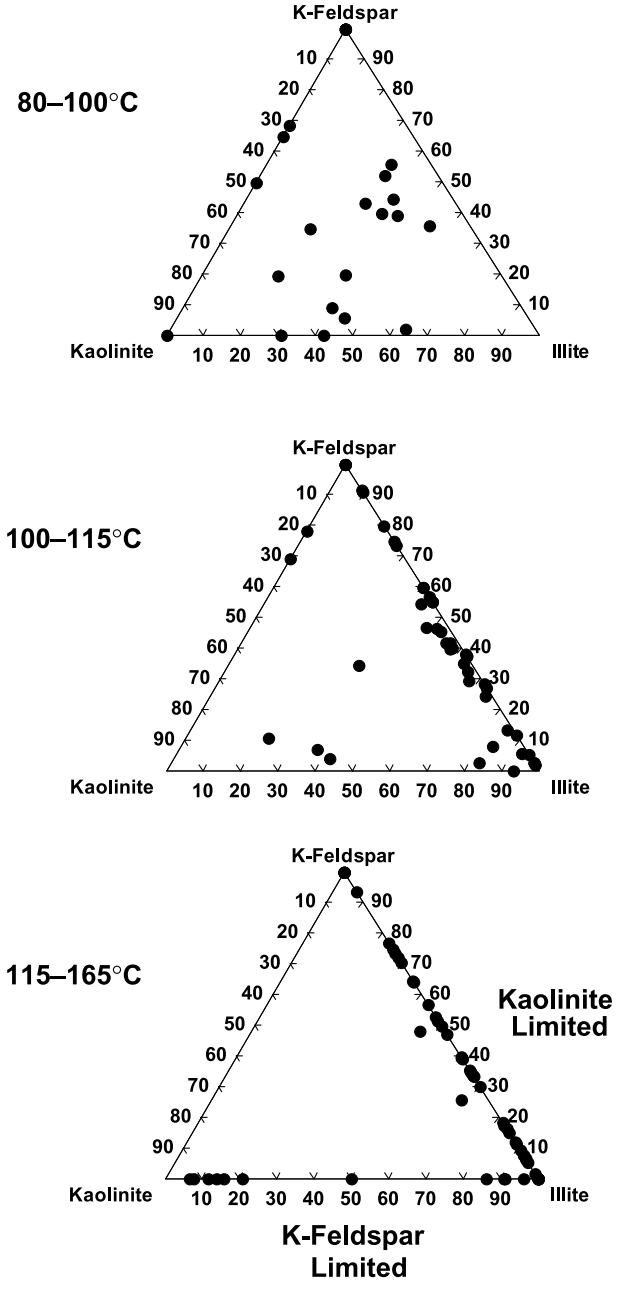

Figure 14. Triangular, normalized plots of reactants (kaolinite and K-feldspar) and product (illite) at different present-day temperatures. The plots show that with increasing temperature, one of the two (or both) reactants is exhausted, resulting in sandstones with either a kaolinite-illite or a K-feldspar-illite assemblage. The former is referred to as feldspar limited and the latter as kaolinite limited.

studies of Aktas and Cocker (1996) and unpublished Aramco internal reports, which describe very thick paleosols near the top of the Unayzah in the shallow fields. Leached K-feldspar associated with pore-filling kaolinite is commonly observed in these intervals. Therefore, the limited supply of K-feldspar for illite formation in the feldspar-limited area may be at least partly due to the kaolinization of K-feldspar during early weathering and influx of meteoric waters near the basin margin.

A provenance effect, in addition to the early leaching effect, cannot yet be excluded from consideration. Differences in original feldspar content are difficult to evaluate due to the effects of early feldspar leaching and deeper conversion to illite. An attempt to evaluate the provenance effect is made by assuming that all kaolinite and illite present in the sandstones have been formed by reaction 1 and that all by-products have been retained in the sandstones. Using this approach, the average reconstructed K-feldspar content is 8% ±4 and 5% ±3 for the kaolinite-limited and feldspar-limited areas, respectively. These means are different at the 95% confidence level. Although it is possible that not all products of K-feldspar alteration were faithfully preserved, these differences suggest that provenance may be a factor. It would indicate that Unayzah sandstones south and southeast of the southern end of Ghawar may have a different provenance than those to the north and west. Both scenarios, early weathering/dissolution and provenance effects, seem likely but require additional evaluation.

TIMING OF DIAGENETIC ILLITE IN THE UNAYZAH

Six samples of Unayzah A eolian dune sandstones were selected from five wells for K/Ar dating of diagenetic illite. Samples from wells A and B are from the feldspar-limited area; samples D, E, and F are from the kaolinite-limited area (Figure 15). All samples were taken from eolian dune facies not affected by pedogenesis. These sandstones have no discernable detrital or infiltrated clays and no detrital mica (petrographically and SEM). Samples A and B contain 6 and 2% kaolinite in thin section and no observable K-feldspar. Wells D, E, and F are from the kaolinite-limited area and contain trace amounts of K-feldspar in thin section (<2%) with no observable kaolinite.

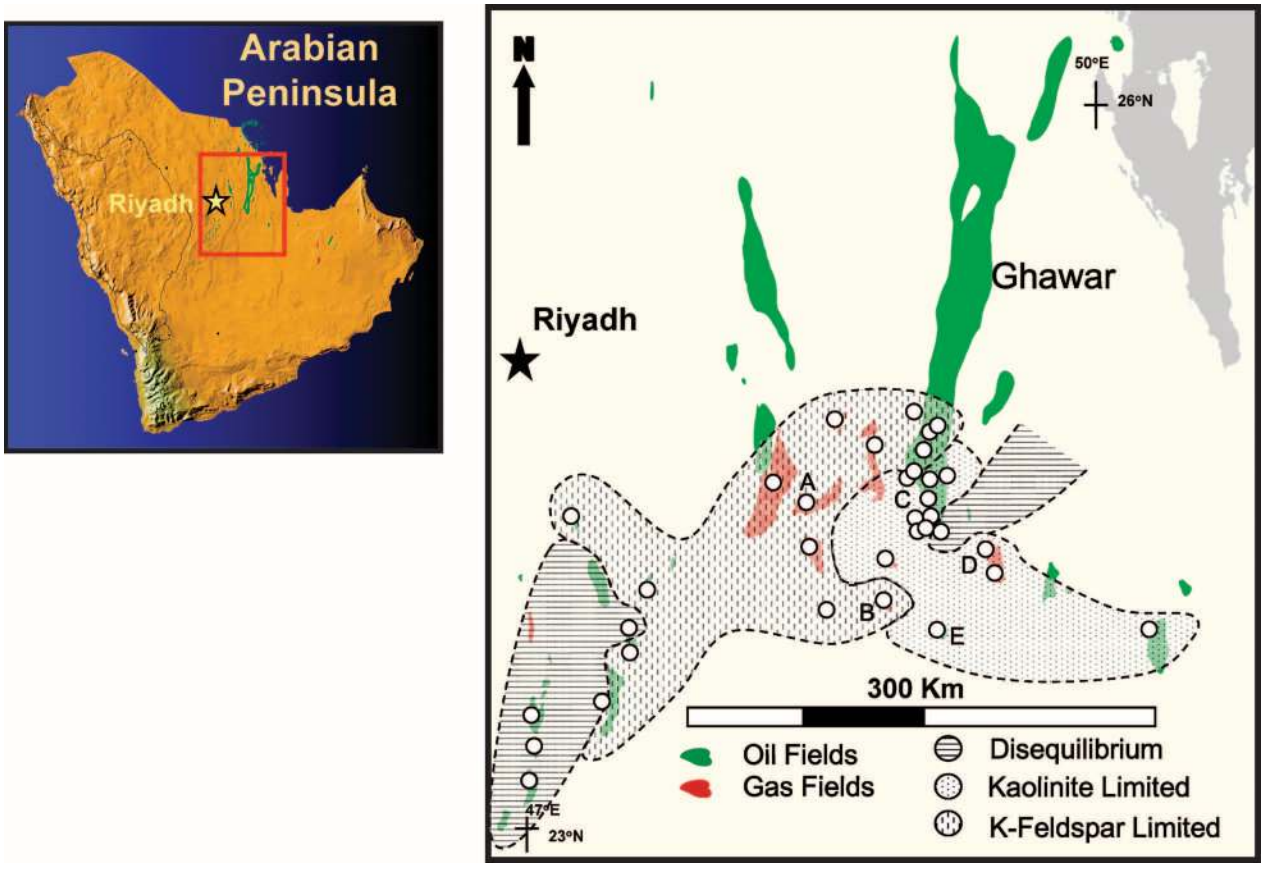

Figure 15. Geographic distribution of wells dominantly consisting of feldspar-limited or kaolinite-limited sandstones and wells with mixtures of kaolinite + illite + K-feldspar (labeled disequilibrium). The single well in the downdip area that is labeled disequilibrium is represented predominantly by samples of low-permeability, very fine sandstones and siltstones.

The clay fractions used for age dating were examined extensively by TEM as well. Most fractions had minor contamination phases composed mainly of quartz and Ti-rich accessory mineral phases, but no K-bearing phases were identified. The prismatic morphologies of the illite laths or plates suggest in-situ neocrystallization. Euhedral particle outlines are typical of an authigenic and diagenetic origin, in contrast to the more irregular or diffuse outlines characteristic of a detrital origin (Clauer and Chaudhuri, 1995).

Ages of diagenetic illite exhibit no systematic differences with illite grain-size fraction (Table 2). Most size fractions less than 2 μm within each sample are identical within analytical error. The 2–6-μm fraction is significantly older in wells A, B, and C, although no evidence of contamination by K-bearing phases was observed. This may reflect an older diagenetic illite component, but in an abundance of caution, this size fraction will be excluded from well-to-well comparisons of the K-Ar ages that follow. Ages of diagenetic illite in the less than 2- and less than 0.4-μm fractions in the six samples exhibit an 11-m.y. spread, ranging from about 98 to 119 Ma, or Early to Late Cretaceous (Cenomanian to Aptian). The ages are referred to the Phanerozoic time scale of Gradstein et al. (2004).

Differences in the mean ages of diagenetic illite may be affected by differences in (1) thermal history, (2) contamination, (3) availability of nucleation sites (surface area), and (4) availability of reactants. A comparison of these factors in the samples examined follows. The less than 0.4-μm fraction is common to all samples and is used as the basis of comparison.

Thermal History

Younger ages may result from more recent exposure to high temperatures creating a younger generation

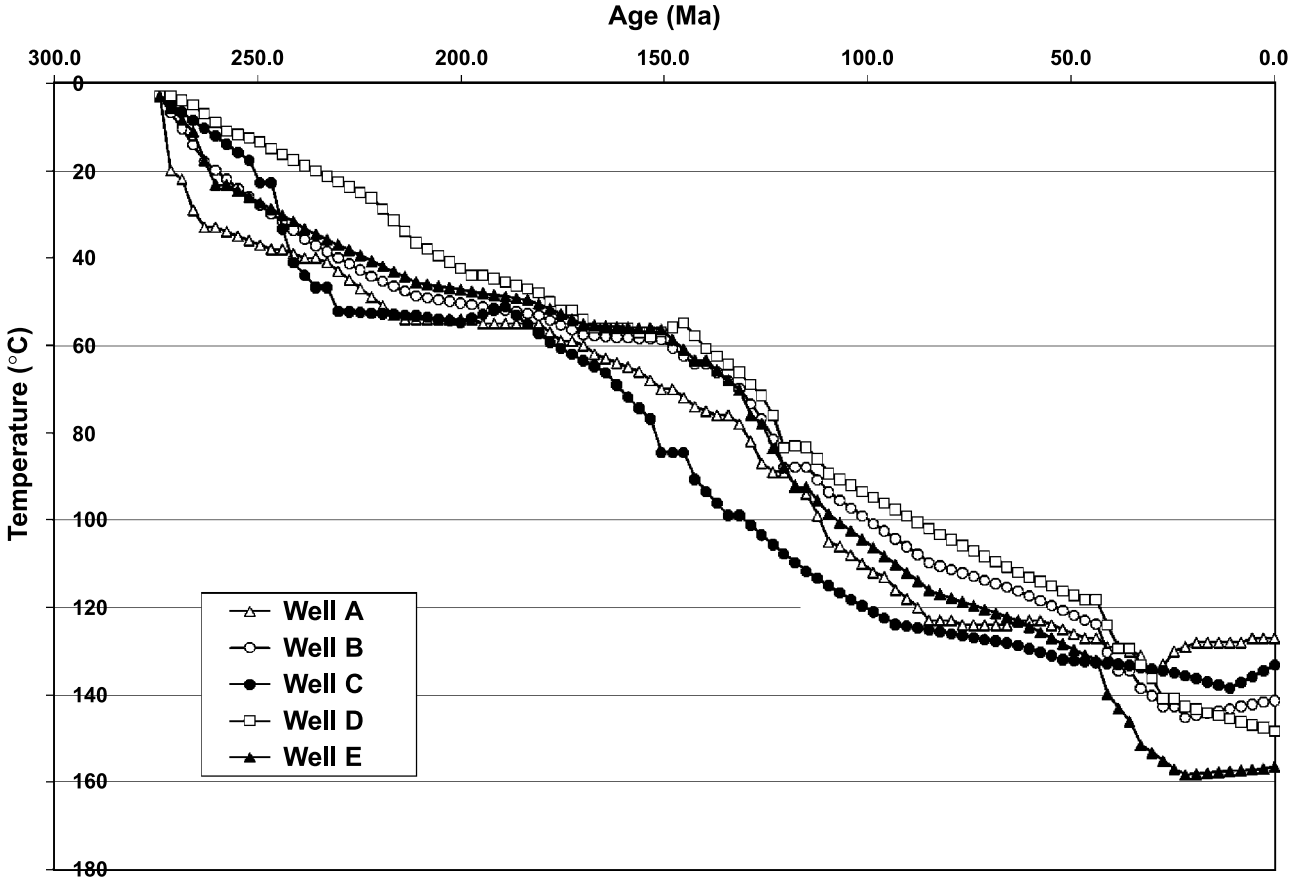

Figure 16. Burial history diagrams of wells A, B, C, D, and E showing time versus temperature.

of diagenetic illite. Figure 16 shows that well E is presently hotter than other wells and has been for about 25 m.y. Its mean K-Ar age, however, is the third oldest (Table 2). Well B, with the second oldest illite ages, also has recent high temperatures. If the thermal history were the only factor accounting for the age differences, then wells that reached illite-generating temperatures earlier should have older ages. Assuming temperatures of approximately 120°C are needed to initiate significant illitization (e.g., Bjorlykke, 1998; Chuhan et al. 2001), Figure 16 shows that well C was the first to reach this temperature and that wells B and D were the last. Well B, however, has older K-Ar ages than either well C or D (Table 2).

Another way of examining the thermal effect is to consider the temperature at the measured time of illite precipitation (mean age). This may possibly reflect any overriding thermal effect. The mean ages from Table 2 and temperatures from the burial history diagram (Figure 16), however, reveal no systematic relation between these two factors. We conclude that the thermal history alone cannot account for the age differences observed.

Contamination

Data have already been presented to rule out contamination as a cause for the age differences. A small percentage (1–3% below XRD detection limit) of Cambrian or older K-feldspar contaminant could shift the measured mean ages a few to several million years, depending on the exact age of the contaminant. However, if K-bearing contaminants were present, they would most likely be present in samples from the areas where remnant K-feldspar is observed (the kaolinite-limited wells C, D, and E). The oldest ages, however, are from samples in which we see no K-feldspar.

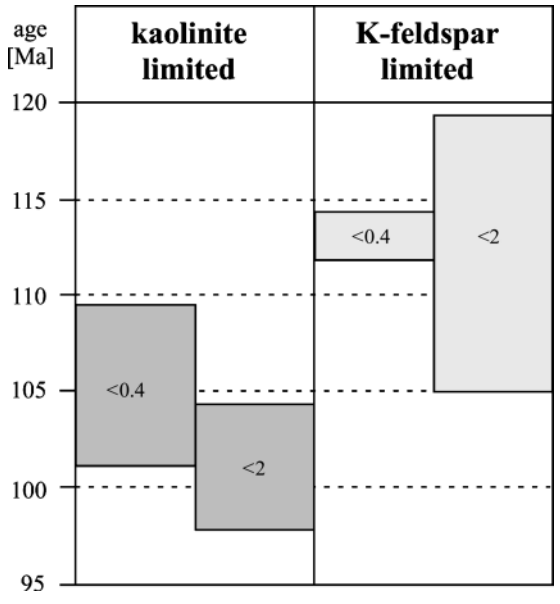

Figure 17. The K-Ar age ranges of illite (1 standard deviation) from the less than 2- and less than 0.4-μm-size fractions of Unayzah sandstones. Ages of feldspar-limited samples are statistically older than those from the kaolinite-limited area. This may be a result of the earlier cessation of illite precipitation in the feldspar-limited area due to smaller amounts of detrital K-feldspar in the original sediment. Continued reaction of more abundant K-feldspar to illite in the kaolinite-limited area eventually consumed all kaolinite but at a later time.

Surface Area

If illite precipitation is affected by the availability of nucleation sites (surface area) as proposed by Lander and Bonnell (2008; 2010, this issue) and in this study (see below), then the initial detrital grain size is a factor in the age of diagenetic illite. Other factors being equal, finer sandstones (more initial surface area) will yield older illite ages than coarser sandstones. The mean grain size of the dated samples in wells A, B, C, D, and E are 0.25, 0.18, 0.13, 0.16, and 0.24 mm (0.009, 0.007, 0.005, 0.006, 0.009 in.), respectively. Based on grain size alone, mean illite ages should be, oldest to youngest, C, D, B, E, and A. An examination of Table 2 shows that this is not the case.

Reactants

Except for the mean illite ages themselves, little information exists regarding when illitization may have ceased in samples where reactants are exhausted. It seems reasonable, however, that sandstones in which a source of potassium is still present (wells C, D, and E) are more likely to have continued to generate illite later than sandstones in which no potassium source remains (wells A and B). Scenarios where this is not the case are possible of course.

Comparing ages of kaolinite-limited and feldspar-limited samples, the less than 0.4-μm fractions from kaolinite-limited samples yield ages ranging from 101 to 109 Ma compared with ages of 112–114 Ma for feldspar-limited samples. A similar difference exists between the less than 2-μm fractions, 98–104 Ma versus 105–119 Ma (Figure 17). Assuming no contamination, these differences suggest that K-feldspar was consumed in the feldspar-limited areas several million years before kaolinite was exhausted in the kaolinite-limited area.

Based on the consideration of the potential factors, which likely would have produced differences in the mean K-Ar ages of diagenetic illite, we tentatively conclude that the differences reflect, at least in part, the time at which either kaolinite or K-feldspar was exhausted and illitization ceased. The number of samples is small, however, and additional dating of illite from these two areas is required to investigate the proposed illitization model in more detail.

An additional factor that was not considered in the foregoing analysis was hydrocarbon effects. Illite ages have commonly been proposed to be affected by hydrocarbon migration or entrapment. Inhibition of illitization in the presence of hydrocarbons and increased illitization due to K-rich brines accompanying hydrocarbon migration have both been proposed (see previous discussion).

A comparison of illite ages in the Unayzah samples we analyzed indicates no systematic relation between hydrocarbons and illite ages. Samples from wells A, D, and E are from within hydrocarbon columns; wells B and C are from nonproductive (wet) zones. Basin modeling suggests that hydrocarbon charge to both productive wells occurred about the same time, a charge of light oil starting approximately 140–150 Ma and with condensate and gas beginning approximately 100 Ma (Arouri

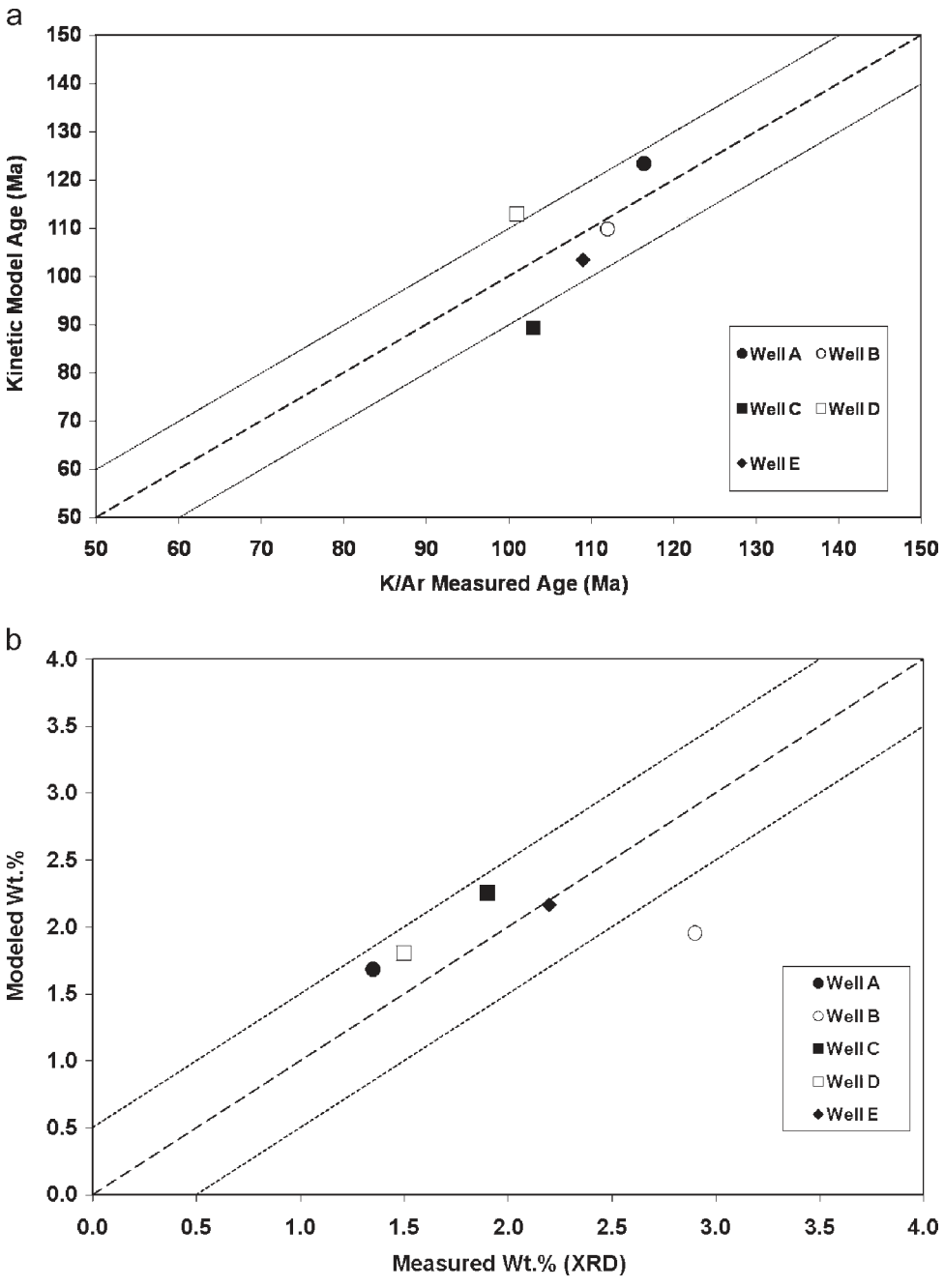

Figure 18. (a) Modeled illite ages versus measured ages based on a simple pseudokinetic model based on the Walderhaug (2000) equation, modified for illite. Even with a fairly simple kinetic model, the agreement between measured and modeled ages is reasonable and compatible with an interpretation of illite precipitation in response to increasing temperature and time. Some modeled ages are greater than measured ages because it was assumed that all samples were not reactant limited. (b) Modeled weight-percent diagenetic illite versus measured weight-percent illite from x-ray diffraction (XRD) analysis. Error bars are shown for the XRD results. The model uses the same kinetic parameters as those used to model ages shown in panel a.

et al. 2009). Illite from the gas condensate column in well A (two samples ~15 ft [4.5 m] apart) yields ages ranging from approximately 113 to 119 Ma for the less than 2- and less than 0.4-µm fractions (Table 2). Illite from the gas or condensate column in well D is dated at 98 and 101 Ma for the less than 2- and less than 0.4-µm fractions, respectively.

Illite from the same-size fractions in the three wet wells (wells B, C, and E) range from 103 to 112 Ma, falling within the spread of ages for the producing wells. No evidence exists that hydrocarbon trapping has inhibited illite formation. This would result in older ages within hydrocarbon-bearing sandstones and younger ages in water-bearing sandstones as, for example, suggested in the classical illite formation model by Lee et al. (1985). Also, there is no compelling evidence that basinal brines accompanying hydrocarbon migration have played a role in illite precipitation as reported in other basins (e.g. Hamilton et al., 1992, North Sea).

MODELING FORMATION OF DIAGENETIC ILLITE IN THE UNAYZAH

Illite precipitation has been modeled using a simplified pseudokinetic approach based on the equations of Walderhaug (2000) for quartz cement. Kinetic parameters, however, have been modified for illite precipitation. Kinetic parameters were chosen to get a best fit between modeled and measured K-Ar ages and weight-percent illite in the five control samples. The same parameters were used for all five simulations (wells A–E). The model can be modified to consider the source of K for illite, the amount of reactants available, and various assumptions about the favorability of nucleation surfaces. However, for this study, the simplest assumptions were selected: (1) the supply of reactants for illite precipitation is unlimited, (2) all grain surfaces are equally receptive to illite precipitation, and (3) precipitation of illite is the rate-limiting step (Altaner, 1986).

The simulation makes it possible to calculate the amount of illite formed and its mean age, assuming continuous growth (no dissolution or reprecipitation). The mean age is calculated by considering the amount of illite formed during each step of the simulation and the mean age of the step. Figure 16 shows the burial history for each well, and Figure 18 shows the modeled ages and amounts of illite for each well.

Although more sophisticated models of illite have recently been developed (e.g., Lander and Bonnell, 2008; 2010, this issue), this rather simple simulation shows that K-Ar ages of illite in the Unayzah are compatible with the gradual growth of illite over geological time with increasing temperatures. Modeled ages and amounts of illite are reasonably close to measured values. The simulated growth over a temperature-time range is compatible with and supported by petrographic observations and by the present depth distribution of illite. Invoking a pulse of hydrothermal fluid, hydrocarbon migration, or a unique thermal event is not necessary. The occurrence of illite, like that of other diagenetic minerals (e.g., quartz cement) in the Unayzah, is a function of availability of reactants, thermal energy, and time.

CONCLUSIONS

Diagenetic illite in Unayzah sandstones forms gradually over time from the reaction of K-feldspar and early diagenetic and detrital kaolinite. The amount of illite is a function of time, temperature, and the relative amounts of K-feldspar and kaolinite in the sandstone prior to illitization. It is limited by the lesser of these two reactants. When either reactant is consumed, illitization ceases. The K/Ar ages of diagenetic illite, therefore, may reflect differences in relative amounts of reactants originally present. Even samples in the same well (same burial history) a few feet apart may give different mean ages because of this effect.

Precipitation of illite and quartz overgrowths overlaps considerably in time, and the two diagenetic minerals compete for nucleation surfaces on uncoated detrital quartz grains. Illite appears to be able to precipitate on all detrital grain surfaces, but it is rarely present on crystal faces of quartz overgrowths. Where diagenetic illite has coated detrital quartz grains, nucleation of quartz overgrowths is inhibited. Therefore, each of these partly coeval cements appears to be able to inhibit the other.

In the Unayzah, no relation between hydrocarbon migration or entrapment and the occurrence or age of diagenetic illite is observed. The observed distribution and timing of diagenetic illite require neither unique thermal nor hydrothermal events. The following petrographic and SEM observations suggest the formation of illite over a time-temperature interval from the reactants kaolinite and K-feldspar: (1) incipient illitization in shallow fields and increasing illitization with increasing depth and temperature, and (2) gradual loss with depth and temperature of reactants K-feldspar and kaolinite accompanied by a corresponding increase in illite.

Provenance and early diagenesis appear to be factors in illite occurrence in the Unayzah. The amounts of diagenetic illite formed depend on (1) the initial amounts of K-feldspar present in the rock and (2) the degree to which K-feldspar is converted to kaolinite during early diagenesis (i.e., the molar proportions of K-feldspar and kaolinite available during deep burial). Sandstones with high initial K-feldspar content may actually produce no

late diagenetic illite under the burial conditions observed in the Unayzah if kaolinite is not available as a co-reactant. At the other extreme, if K-feldspar is absent, either because of provenance or removal during early diagenesis, then little or no late diagenetic illite is formed. These conclusions are very similar to those of Chuhan et al. (2000) in their study of illite in the North Sea.

In the Unayzah, illite precipitation is favored in sandstones in which K-feldspar somewhat exceeded kaolinite prior to deep burial. Sandstones with initially high K-feldspar content appear to be mostly south-southeast of the southern end of the Ghawar structure; those with lower amounts of K-feldspar and those that underwent a higher degree of kaolinization are mostly to the west-southwest.

REFERENCES CITED

Aase, N. E., P. A. Bjorkum, and P. H. Nadeau, 1996, The effect of grain-coating microquartz on preservation of reservoir porosity: AAPG Bulletin, v. 80, p. 1654–1673.

Aktas, G., and J. D. Cocker, 1996, Diagenetic and depositional controls on reservoir quality in Khuff and Unayzah sandstones, Hawtah trend, central Saudi Arabia: Geo '94: The Middle East Petroleum Geosciences, v. 1, p. 44–52.

Altaner, S. P., 1986, Comparison of rates of smectite illitization with rates of K-feldspar dissolution: Clays and Clay Minerals, v. 34, p. 608–611, doi:10.1346/CCMN.1986.0340517.

Arouri, K. R., S. H. Al-Saleh, and Z. M. Al-Hilal, 2009, Residual oil as a tool in migration and filling history analysis of petroleum reservoirs, Ghazal field, Saudi Arabia: Organic Geochemistry, v. 40, p. 617–627, doi:10.1016/j.orggeochem.2009.02.002.

Bjorkum, P. A., and N. Gjelsvik, 1988, An isochemical model for the formation of authigenic kaolinite, K-feldspar and illite in sediments: Journal of Sedimentary Research, v. 58, p. 506–511.

Bjorlykke, K., 1998, Clay mineral diagenesis in sedimentary basins—A key to the prediction of rock properties: Clay Minerals, v. 33, p. 15–34, doi:10.1180/000985598545390.

Bonhomme, M. G., R. Thuizat, Y. Pinault, N. Clauer, R. Wendling, and R. Winkler, 1975, Methode de datation potassium-argon, Appareillage et technique: Strasbourg, Notes Tech. Inst. Geol., Univ. Louis Pasteur, 53 p.

Chuhan, F., K. Bjorlykke, and C. Lowrey, 2000, The role of provenance in illitization of deeply buried reservoir sandstones from Haltenbanken and north Viking Graben, offshore Norway: Marine and Petroleum Geology, v. 17, p. 673–689, doi:10.1016/S0264-8172(00)00014-3.

Chuhan, F., K. Bjorlykke, and C. Lowrey, 2001, Closed system burial diagenesis in reservoir sandstones: Examples from the Garn Formation at Haltenbanken area, offshore mid-Norway: Journal of Sedimentary Research, v. 71, p. 15–26, doi:10.1306/041100710015.

Clauer, N., and S. Chaudhuri, 1995, Clays and crustal cycles: Heidelberg, New York, Springer-Verlag, 359 p.

Clauer, N., J. D. Cocker, and S. Chaudhuri, 1992, Isotopic dating of diagenetic illites in reservoir sandstones: Influence of the investigator effect, *in* D. W. Houseknecht and E. D. Pittman, eds., Origin, diagenesis, and petrophysics of clay minerals: SEPM Special Publication 47, p. 5–12.

Dalrymple, G. B., and M. A. Lanphere, 1969, Potassium-argon dating: San Francisco, W. H. Freeman, 258 p.

Eberl, D. D., and J. Środoń, 1988, Ostwald ripening and interparticle-diffraction effects for illite crystals: American Mineralogist, v. 73, p. 1335–1345.

Eberl, D. D., J. Środoń, M. Kralik, B. E. Taylor, and Z. E. Peterman, 1990, Ostwald ripening of clays and metamorphic minerals: Science, v. 248, p. 474–477.

Ehrenberg, S. N., and P. Nadeau, 1989, Formation of diagenetic illite in sandstones of the Garn Formation, Haltebanken, mid-Norwegian continental shelf: Clay Minerals, v. 24, p. 233–253, doi:10.1180/claymin.1989.024.2.09.

Faure, G., 1986, Principles of isotope geology: New York, John Wiley & Sons, 589 p.

Franks, S. G., 2008, From plate to pore: Plate movement, paleoclimate, paleosols, and the effects of early clay and microquartz grain coatings on deep porosity in Permo-Carboniferous Unayzah sandstone, Saudi Arabia (abs.): International AAPG Meeting, Capetown, http://www.searchanddiscovery.net/abstracts/html/2008/intl_capetown/abstracts/471894.htm (accessed August 2009).

Garming, J. F. L., S. G. Franks, H. Cremer, and O. A. Abbink, 2010, Biogenic silica microfossils in sediments of the Permian–Carboniferous Unayzah Formation, Saudi Arabia: GeoArabia, v. 15, p. 119–132.

Gaupp, R., A. Matter, J. Platt, K. Ramsayer, and J. Walzebruck, 1993, Diagenesis and fluid evolution of deeply buried Permian (Rotliegende) gas reservoirs, northwest Germany: AAPG Bulletin, v. 77, p. 1111–1128.

Gluyas, J. G., and A. Leonard, 1995, Diagenesis of the Rotliegende sandstone: The answer "ain't blowin" in the wind: Marine and Petroleum Geology, v. 12, p. 491–497, doi:10.1016/0264-8172(95)91504-I.

Gradstein, F., J. Ogg, and A. Smith, 2004, A geologic time scale 2004: Cambridge, Cambridge University Press, 589 p.

Grathoff, G. H., D. M. Moore, R. L. Hay, and K. Wemmer, 2001, Origin of illite in the lower Paleozoic of the Illinois basin: Evidence for brine migration: Geological Society of America Bulletin, v. 113, p. 1092–1104, doi:10.1130/0016-7606(2001)113<1092:OOIITL>2.0.CO;2.

Hamilton, P. J., S. Kelley, and A. E. Fallick, 1989, K-Ar dating of illite in hydrocarbon reservoirs: Clays and Clay Minerals, v. 24, p. 215–231.

Hamilton, P. J., M. R. Giles, and P. Ainsworth, 1992, K-Ar dating of illites Brent Group reservoirs: A regional perspective, *in* A. C. Morton, R. S. Haszeldine, M. R. Giles,

and S. Brown, eds., Geology of the Brent Group: Geological Society (London) Special Publication 61, p. 377–400.
Hancock, N. J., and A. M. Taylor, 1978, Clay mineral diagenesis and oil migration in the Middle Jurassic Brent Sand Formation: Journal of the Geological Society (London), v. 135, p. 69–72, doi:10.1144/gsjgs.135.1.0069.
Jourdan, A., M. Thomas, O. Brevart, P. Robson, F. Sommer, and M. Sullivan, 1987, Diagenesis as the control of the Brent sandstone reservoir in the Greater Alwyn area (east Shetland Basin), *in* J. Brooks and K. W. Glennie, eds., Petroleum geology of N.W. Europe: London, Graham & Trotman, p. 951–961.
Lander, R. H., and L. M. Bonnell, 2008, Prediction of fibrous illite and associated secondary porosity formation in sandstones (abs.): AAPG Annual Meeting Abstracts, v. 17, p.115.
Lander, R. H., and L. M. Bonnell, 2010, A model for fibrous illite nucleation and growth in sandstones: AAPG Bulletin, v. 94, p. 1161–1187, doi:10.1306/04211009121.
Lee, M., 1984, Diagenesis of the Permian Rotliegendes sandstone, North Sea: K/Ar, $^{18}O/^{16}O$, and petrologic evidence: Ph.D. thesis, Case Western Reserve University, Cleveland, Ohio, 365 p.
Lee, M., J. L. Aronson, and S. M. Savin, 1985, K/Ar dating of Rotliegende sandstone, Netherlands: AAPG Bulletin, v. 69, p. 1381–1385.
Lee, M., J. L. Aronson, and S. M. Savin, 1989, Timing and conditions of Permian Rotliegendes sandstone diagenesis, southern North Sea: K/Ar and oxygen isotopic data: AAPG Bulletin, v. 73, p. 195–215.
Liewig, N., N. Clauer, and F. Sommer, 1987, Rb-Sr and K-Ar dating of clay diagenesis in Jurassic sandstone oil reservoirs: North Sea: AAPG Bulletin, v. 71, p. 1467–1474.
Mack, G. H., W. C. James, and H. C. Monger, 1993, Classification of paleosols: Geological Society of America Bulletin, v. 106, p. 129–136, doi:10.1130/0016-7606(1993)105<0129:COP>2.3.CO;2.
McDougall, I., and Z. Roksandic, 1974, Total fusion $^{40}Ar/^{39}Ar$ ages using HIFAR reactor: Journal of the Geological Society of Australia, v. 21, p. 81–89.
Melvin, J., and R. Sprague, 2006, Advances in Arabian stratigraphy: Origin and stratigraphic architecture of glaciogenic sediments in Permian–Carboniferous lower Unayzah sandstones, eastern central Saudi Arabia: GeoArabia, v. 11, p. 105–152.
Meunier, A., and B. Velde, 2004, Illite: Origins, evolution and metamorphism: Berlin, Springer, 286 p.
Meunier, A., B. Velde, and P. Zalba, 2004, Illite K-Ar dating and crystal growth processes in diagenetic environments: A critical review: Terra Nova, v. 16, p. 296–304, doi:10.1111/j.1365-3121.2004.00563.x.
Moore, D. A., and J. R. Reynolds, 1997, X-ray diffraction and the identification and analysis of clay minerals: Oxford, Oxford University Press, 378 p.
Murr, L. E., 1982, Electron and ion microscopy and microanalysis—Principles and applications, optical engineering, v. 1: New York, Marcel Dekker, 793 p.
Pevear, D. R., 1999, Illite and hydrocarbon exploration: Proceedings of the National Academy of Science, U.S.A., v. 96, p. 3440–3446.
Platt, J. D., 1993, Controls on clay mineral distribution and chemistry in the Early Permian Rotliegende of Germany: Clay Minerals, v. 28, p. 393–416, doi:10.1180/claymin.1993.028.3.05.
Robinson, A. G., M. L. Coleman, and J. G. Gluyas, 1993, The age of illite cement growth, Village fields area, southern North Sea: Evidence from K-Ar ages and $^{18}O/^{16}O$ ratios: AAPG Bulletin, v. 77, p. 68–80.
Rossel, N. C., 1982, Clay mineral diagenesis in Rotliegende eolian sandstones of the southern North Sea: Clay Minerals, v. 17, p. 69–77, doi:10.1180/claymin.1982.017.1.07.
Senalp, M., and A. Al-Duaiji, 2001, Sequence stratigraphy of the Unayzah reservoir in central Saudi Arabia: The Saudi Aramco Journal of Technology, p. 20–43.
Shammari, S., and K. Shahab, 2002, The role of micro-quartz cementation in porosity preservation in deep Paleozoic sandstone reservoirs, Saudi Arabia (abs.): AAPG International Convention, Cairo, http://www.searchanddiscovery.net/documents/abstracts/cairo2002/images/shammari.htm (accessed August 2009).
Sommer, F., 1978, Diagenesis of Jurassic sandstones in the Central Graben: Journal of the Geological Society (London), v. 135, p. 63–67, doi:10.1144/gsjgs.135.1.0063.
Środoń, J., D. D. Eberl, and V A. Drits, 2000, Evolution of fundamental-particle size during illitization of smectite and implications for reaction mechanism: Clays and Clay Minerals, v. 48, p. 446–458, doi:10.1346/CCMN.2000.0480405.
Steiger, R. H., and E. Jäger, 1977, Subcommission on Geochronology: Convention on the use of decay constants in geo- and cosmochronology: Earth and Planetary Science Letters, v. 36, p. 359–362.
Sudo, T., S. Shimoda, H. Yotusumoto, and S. Aita, 1981, Electron micrographs of clay minerals: Developments in Sedimentology, v. 31: Amsterdam, Oxford, New York, Elsevier, 203 p.
Turner, P., M. Jones, D. J. Prosser, G. D. Williams, and A. Searl, 1993, Structural and sedimentologic controls on diagenesis in a Rotliegende gas reservoir (Ravenspur North), U.K. southern North Sea, *in* J. R. Parker, ed., Petroleum geology of northwest Europe: Proceedings of the 4th Conference: Geological Society (London), p. 771–785.
Walderhaug, O., 2000, Modeling quartz cementation and porosity in Middle Jurassic Brent Group sandstones of the Kvitebjorn field, northern North Sea: AAPG Bulletin, v. 84, p. 1325–1339.
Worden, R., and S. Morad, 2003, Clay mineral cements in sandstones: International Association of Sedimentologists Special Publication 34, 509 p.
Ziegler, K., 1993, Diagenetic and geochemical history of the Rotliegende of the southern North Sea (U.K. Sector): A comparative study: Ph.D. thesis, Reading University, United Kingdom.
Ziegler, K., 2006, Clay minerals of the Permian Rotliegende Group in the North Sea and adjacent areas: Clay Minerals, v. 41, p. 355–393, doi:10.1180/0009855064110200.

Ziegler, K., B. W. Sellwood, and A. E. Fallick, 1994, Radiogenic and stable isotope evidence for age and origin of authigenic illites in the Rotliegende, southern North Sea: Clay Minerals, v. 29, p. 555–565, doi:10.1180/claymin.1994.029.4.12.

Zwingmann, H., N. Clauer, and R. Gaupp, 1998, Timing of fluid flow in a sandstone reservoir of the north German Rotliegende (Permian) by K-Ar dating of related hydrothermal illite: Geological Society (London) Special Publication 144, p. 91–106.

Zwingmann, H., N. Clauer, and R. Gaupp, 1999, Structural related geochemical (REE) and isotopic characteristics (K-Ar, Rb-Sr, δ18O) characteristics of clay minerals from Rotliegende sandstone reservoirs (Permian, northern Germany): Geochimica et Cosmochemica Acta, v. 63, p. 2805–2823, doi:10.1016/S0016-7037(99)00198-2.